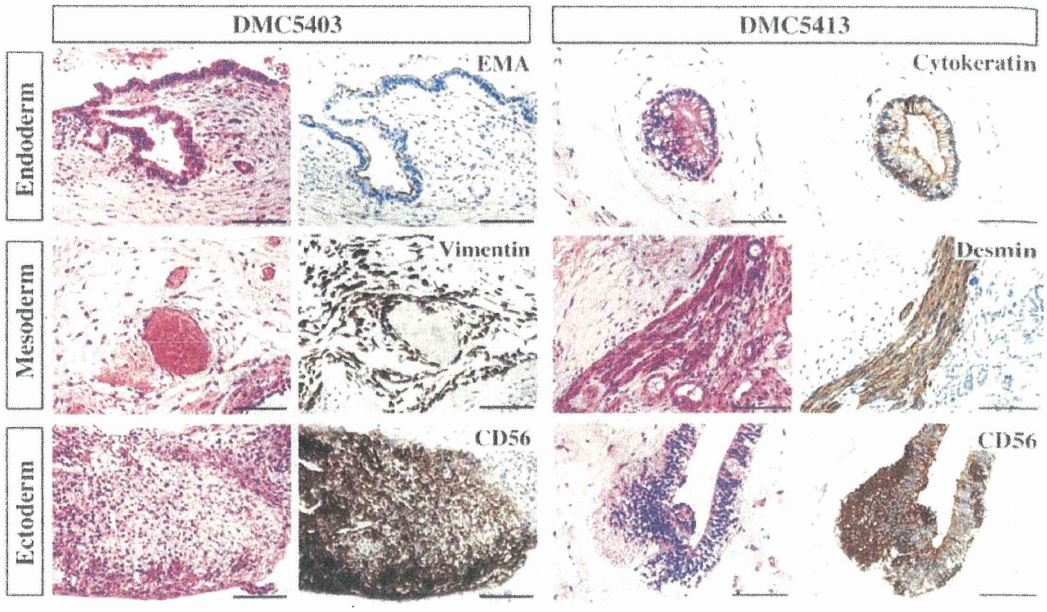

Figure 6. In vivo differentiation of DMC-hiPSCs. Teratomas derived from two DMC-hiPSCs (DMC5403, DMC5413) were examined by H&E and immunohistochemical staining. Teratomas from both DMC-hiPSCs contained histological components of the three germ layers, including neuroepithelial structures expressing human neural cell adhesion molecule (NCAM) (CD56, ectoderm), blood vessels and fibrous stroma-like structures expressing human vimentin or muscle-like structures expressing desmin (mesoderm), and gut-like epithelium expressing epithelial membrane antigen (EMA) or AE1 and AE3 (endoderm). Scale bars: 100 μm.

pluripotent stem cell markers), and DNA methylation status of the OCT3/4 and NANOG promoters, although these iPSC clones showed minor differences from each other in gene expression patterns and in the methylation status of promoter regions. In addition, the DMC-hiPSCs were able to differentiate into components of the three germ layers in vitro and in vivo. These data indicated that the DMC-hiPSC clones acquired full pluripotency equal to that of hiPSCs derived from DFBs or other cell sources and that the generation of iPSCs from DMCs is feasible.

The overall efficiency of reprogramming DMCs was almost the same as for DFBs, the most commonly used primary cell type for generating hiPSCs. However, we found several differences between DMCs and DFBs in the present study. In comparison with DFBs, DMCs formed about half the number of ALP^+ colonies (Fig. 2B, top). However, about 90% of the hESC-like colonies from DMCs were fully reprogrammed, while fewer than 40% of those from DFBs were successfully reprogrammed (Fig. 2B, bottom). Consequently, the overall reprogramming efficiency of DMCs was comparable to that of DFBs. There are various possible reasons for this higher reprogramming efficiency of DMCs. First, given that DMCs expressed the amphotropic retrovirus-introduced transgenes at two to three times the level expressed by DFBs (Fig. 2A), DMCs may be particularly compatible with this gene transduction system. Second, the endogenous gene expression profile of DMCs might result in improved reprogramming efficiency. Many previous reports have indicated that OSKM are important for reprogramming cells to iPSCs and that the endogenous expression of any of the four factors can reduce the number of genes needed for reprogramming (6,19,35). Furthermore, recently reported key molecules for efficient reprogramming, MYCL1 and GLIS1 (24,36), were expressed by the DMCs.

Our quantitative RT-PCR analysis showed that, among the four reprogramming factors (OSKM), only c-MYC was expressed in DMCs at the same level as in hESCs, similar to other placenta-derived cells and DFBs (Fig. 1). However, expression of the GLIS1 gene was detected only in the testis, placenta, and their derivative cells, the AECs and DMCs (Fig. 8). The transduction of GLIS1 along with OCT3/4, KLF4, and SOX2 markedly increases the expression of several genes that enhance iPSC generation, including lin-28 homolog A (*C. elegans*; LIN28A) (47), NANOG (38), neuroblastoma-derived Myc (MYCN), and MYCL1 (31), and the number of fully reprogrammed cells (24). The low endogenous expression of GLIS1 in the DMCs, combined with the efficient retroviral gene transduction, might contribute to the higher efficiency of DMC reprogramming.

On the other hand, the level of MYCL1 expression in the three placenta-derived cell types was low compared to that in DFBs (Fig. 8A). It is well known that DFBs can be reprogrammed efficiently by three (OSK)

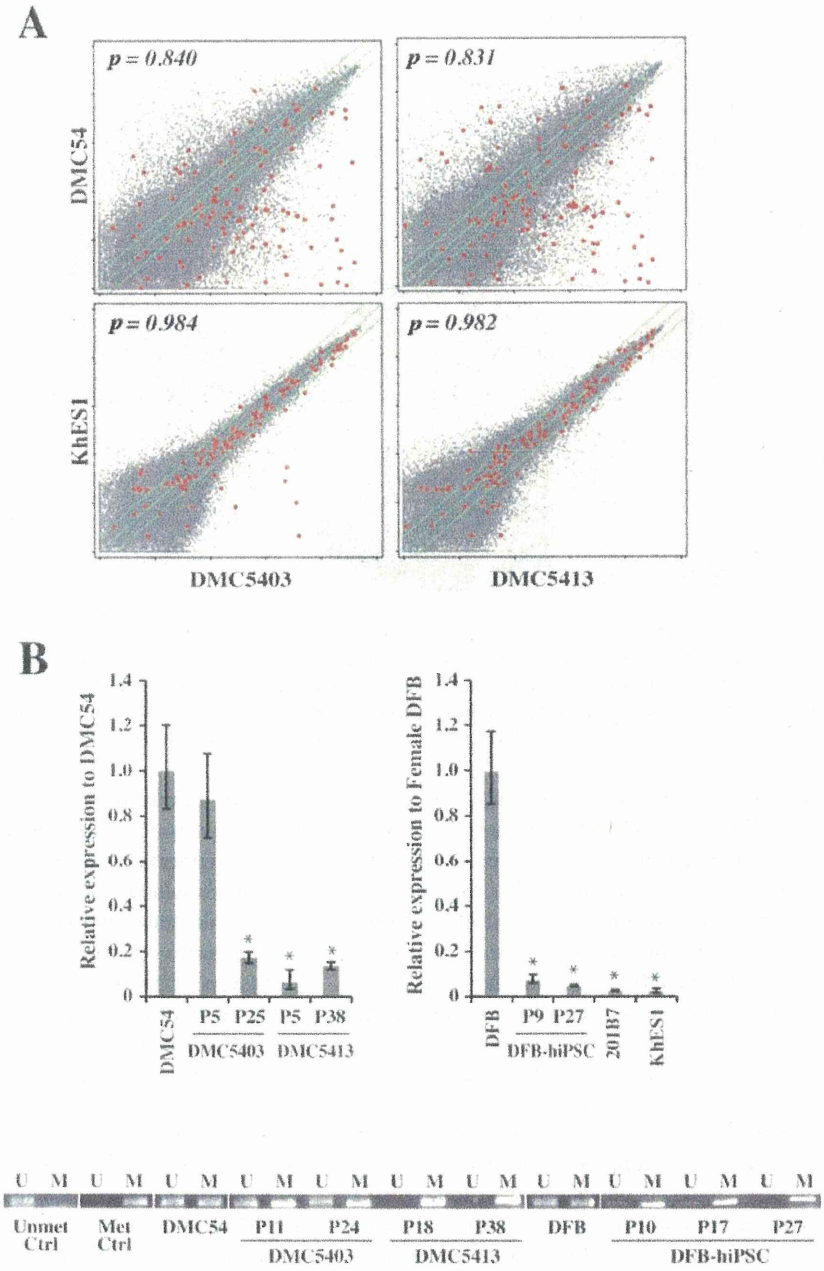

Figure 7. Transcriptional expression analysis of DMC-hiPSCs. (A) Scatter plots comparing the DNA microarray analysis data between DMC-iPSCs and parental DMCs (top) and between DMC-hiPSCs and human ES cells (KhES1) (bottom). The diagonal lines indicate twofold changes between the two samples, and the Pearson's coefficients are shown in the scatter plots. Red dots indicate data from probe sets for characterizing undifferentiated stem cells (see Table 1). (B) qRT-PCR analysis of X (inactive)-specific transcript (XIST) gene expression in female cells. Data are presented as the value relative to parental DMCs or DFBs. (C) Methylation-specific PCR was performed to examine the methylation status of the XIST promoter. The PCR products were specific for the methylated (M) or unmethylated (U) genome.

Table 3. Gene Expression Data of the Probe Sets in the Affymetrix Human Genome U133 Plus 2.0 Array for the Characterization of Undifferentiated Stem Cells

				Flag[a]				Fold Change Versus DMC54		Fold Change Versus KhES1	
Probe Set ID	UniGene ID	Gene Title	Symbol	DMC54	DMC5403	DMC5413	KhES1	DMC5403	DMC5413	DMC5403	DMC5413
1552982_a_at	Hs.1755	Fibroblast growth factor 4	FGF4	A	A	A	A	1.8	2.6	1.5	2.2
1554776_at	Hs.335787	Zinc finger protein 42 homolog (mouse)	ZFP42	A	P	P	P	84.4	75.3	−1.2	−1.4
1554777_at	Hs.335787	Zinc finger protein 42 homolog (mouse)	ZFP42	A	P	P	P	126.1	220.4	−1.5	1.2
1555271_a_at	Hs.492203	Telomerase reverse transcriptase	TERT	A	A	A	M	4.1	3.0	1.1	−1.2
1560469_at	Hs.33446	Nuclear receptor subfamily 5, group A, member 2	NR5A2	A	P	A	A	33.0	2.7	11.4	−1.1
1569689_s_at	Hs.302352	γ-Aminobutyric acid (GABA) A receptor, β3	GABRB3	A	A	A	A	1.6	−1.3	1.6	−1.3
201005_at	Hs.114286	CD9 molecule	CD9	P	P	P	P	2.2	2.8	1.1	1.4
201315_x_at	Hs.709321	Interferon-induced transmembrane protein 2 (1-8D)	IFITM2	P	P	P	P	−1.6	−1.2	1.5	1.9
201578_at	Hs.723993	Podocalyxin-like	PODXL	P	P	P	P	8.7	7.8	1.2	1.1
201601_x_at	Hs.458414	Interferon-induced transmembrane protein 1 (9-27)	IFITM1	P	P	P	P	3.9	4.5	1.7	1.9
202575_at	Hs.405662	Cellular retinoic acid binding protein 2	CRABP2	A	P	P	P	7.5	25.7	−2.7	1.3
204053_x_at	Hs.500466	Phosphatase and tensin homolog	PTEN	P	P	P	P	−1.3	−1.3	1.0	1.0
204054_at	Hs.500466	Phosphatase and tensin homolog	PTEN	P	P	P	P	−2.2	−2.1	−1.0	1.0
204271_s_at	Hs.82002	Endothelin receptor type B	EDNRB	A	P	P	P	596.2	435.3	2.2	1.6
204273_at	Hs.82002	Endothelin receptor type B	EDNRB	A	P	P	P	514.5	609.4	2.8	3.3
204535_s_at	Hs.631513	RE1-silencing transcription factor	REST	A	A	A	A	−3.2	−1.1	−1.1	2.7
204863_s_at	Hs.532082	Interleukin 6 signal transducer (gp130, oncostatin M receptor)	IL6ST	P	A	A	A	−11.8	−7.5	−1.4	1.1
204864_s_at	Hs.532082	Interleukin 6 signal transducer (gp130, oncostatin M receptor)	IL6ST	P	A	A	P	−10.1	−1.2	−7.3	1.1
205051_s_at	Hs.479754	v-Kit Hardy-Zuckerman 4 feline sarcoma viral oncogene homolog	KIT	P	P	P	P	9.1	10.8	−1.6	−1.4
205603_s_at	Hs.226483	Diaphanous homolog 2 (Drosophila)	DIAPH2	P	P	P	P	29.9	17.6	1.3	−1.3
205726_at	Hs.226483	Diaphanous homolog 2 (Drosophila)	DIAPH2	P	P	P	P	4.2	4.1	1.0	−1.0
205850_s_at	Hs.302352	γ-Aminobutyric acid (GABA) A receptor, β3	GABRB3	A	P	P	P	44.4	50.6	−1.4	−1.2
205876_at	Hs.133421	Leukemia inhibitory factor receptor α	LIFR	A	P	A	P	3.4	1.5	−1.0	−2.3
206012_at	Hs.520187	Left-right determination factor 2	LEFTY2	A	P	P	P	970.9	465.7	1.1	−1.9
206268_at	Hs.724790	Left-right determination factor 1	LEFTY1	A	P	P	P	342.1	155.5	1.2	−1.8
206286_s_at	Hs.385870	Teratocarcinoma-derived growth factor 1 teratocarcinoma-derived growth factor 3, pseudogene	TDGF1 TDGF3	A	P	P	P	12405.4	9524.5	1.4	1.1
206701_x_at	Hs.82002	Endothelin receptor type B	EDNRB	A	P	P	P	197.9	108.6	2.7	1.5
206783_at	Hs.1755	Fibroblast growth factor 4	FGF4	A	P	P	P	24.5	31.9	1.1	1.5
206805_at	Hs.252451	Sema domain, immunoglobulin domain (Ig), short basic domain, secreted, (semaphorin) 3A	SEMA3A	P	P	P	P	2.4	1.2	1.3	−1.4
207199_at	Hs.492203	Telomerase reverse transcriptase	TERT	A	P	P	P	3.0	3.9	−1.8	−1.4

(*continued*)

Table 3. Gene Expression Data of the Probe Sets in the Affymetrix Human Genome U133 Plus 2.0 Array for the Characterization of Undifferentiated Stem Cells (*Continued*)

				Flag[a]				Fold Change Versus DMC54		Fold Change Versus KhES1	
Probe Set ID	UniGene ID	Gene Title	Symbol	DMC54	DMC5403	DMC5413	KhES1	DMC5403	DMC5413	DMC5403	DMC5413
207466_at	Hs.278959	Galanin prepropeptide	GAL	A	P	P	P	28.6	12.6	1.5	–1.5
207545_s_at	Hs.654609	Numb homolog (Drosophila)	NUMB	P	P	P	P	1.1	1.2	1.9	2.0
207742_s_at	Hs.586460	Nuclear receptor subfamily 6, group A, member 1	NR6A1	A	A	A	A	11.4	19.9	–2.2	–1.2
208275_x_at	Hs.458406	Undifferentiated embryonic cell transcription factor 1	UTF1	A	P	P	P	13.0	29.6	1.1	2.5
208286_x_at	Hs.632482	POU class 5 homeobox 1 POU class 5 homeobox 1B POU class 5 homeobox 1 pseudogene 3 POU class 5 homeobox 1 pseudogene 4	POU5F1 POU5F1B POU5F1P3 POU5F1P4	A	P	P	P	1925.3	2025.3	1.1	1.2
208337_s_at	Hs.33446	Nuclear receptor subfamily 5, group A, member 2	NR5A2	A	P	P	P	37.8	26.4	1.0	–1.4
208343_s_at	Hs.33446	Nuclear receptor subfamily 5, group A, member 2	NR5A2	A	P	P	P	153.3	39.3	1.4	–2.7
208378_x_at	Hs.37055	Fibroblast growth factor 5	FGF5	P	A	A	A	–9.8	–55.8	1.9	–3.0
208500_x_at	Hs.546573	Forkhead box D3	FOXD3	A	A	A	A	5.5	14.1	–7.9	–3.1
209073_s_at	Hs.654609	Numb homolog (Drosophila)	NUMB	P	P	P	P	–1.2	1.1	1.1	1.4
210002_at	Hs.514746	GATA binding protein 6	GATA6	P	A	A	A	–38.1	–4.8	–1.3	6.0
210174_at	Hs.33446	Nuclear receptor subfamily 5, group A, member 2	NR5A2	A	P	P	P	28.8	9.6	2.3	–1.3
210310_s_at	Hs.37055	Fibroblast growth factor 5	FGF5	P	A	A	A	–127.2	–102.7	–1.4	–1.1
210311_at	Hs.37055	Fibroblast growth factor 5	FGF5	P	A	M	A	–4.5	–6.8	1.6	1.0
210391_at	Hs.586460	Nuclear receptor subfamily 6, group A, member 1	NR6A1	A	A	A	A	1.5	4.1	–1.5	1.7
210392_x_at	Hs.586460	Nuclear receptor subfamily 6, group A, member 1	NR6A1	A	M	A	A	6.7	6.1	1.2	1.1
210560_at	Hs.184945	Gastrulation brain homeobox 2	GBX2	A	A	A	A	4.5	10.3	3.6	8.4
210761_s_at	Hs.86859	Growth factor receptor-bound protein 7	GRB7	A	P	P	P	1.6	3.2	–1.3	1.5
211000_s_at	Hs.532082	Interleukin 6 signal transducer (gp130, oncostatin M receptor)	IL6ST	P	A	A	A	–8.2	–7.5	1.3	1.5
211402_x_at	Hs.586460	Nuclear receptor subfamily 6, group A, member 1	NR6A1	A	A	A	A	13.6	10.7	–1.0	–1.3
211711_s_at	Hs.500466	Phosphatase and tensin homolog	PTEN	P	P	P	P	–1.8	–2.2	1.0	–1.2
212195_at	Hs.532082	Interleukin 6 signal transducer (gp130, oncostatin M receptor)	IL6ST	P	P	P	P	–17.9	–15.2	1.2	1.4
212196_at	Hs.532082	Interleukin 6 signal transducer (gp130, oncostatin M receptor)	IL6ST	P	P	P	P	–4.2	–3.7	1.1	1.3
212920_at	Hs.631513	RE1-silencing transcription factor	REST	P	P	P	P	1.5	2.4	–1.1	1.4
213721_at	Hs.518438	SRY (sex-determining region Y)-box 2	SOX2	A	P	P	P	72.0	53.6	1.1	–1.3
213722_at	Hs.518438	SRY (sex-determining region Y)-box 2	SOX2	A	A	A	A	9.6	2.9	1.4	–2.3
214022_s_at	Hs.458414	Interferon-induced transmembrane protein 1 (9-27)	IFITM1	P	P	P	P	5.7	6.1	1.7	1.8

Probe Set ID	UniGene ID	Gene Title	Symbol	Flag[a]				Fold Change Versus DMC54		Fold Change Versus KhES1	
				DMC54	DMC5403	DMC5413	KhES1	DMC5403	DMC5413	DMC5403	DMC5413
214178_s_at	Hs.518438	SRY (sex-determining region Y)-box 2	SOX2	A	A	A	A	4.3	3.3	1.4	1.1
214218_s_at	Hs.730656	X (inactive)-specific transcript (nonprotein coding)	XIST	P	P	P	P	−1.0	−60.2	80.1	1.4
214240_at	Hs.278959	Galanin prepropeptide	GAL	A	P	P	P	3871.9	2443.0	1.6	−1.0
217246_s_at	Hs.226483	Diaphanous homolog 2 (Drosophila)	DIAPH2	A	A	A	P	1.4	1.2	−1.1	−1.3
218048_at	Hs.720384	COMM domain containing 3	COMMD3	P	P	P	P	−5.1	−9.7	1.3	−1.4
218847_at	Hs.35354	Insulin-like growth factor 2 mRNA binding protein 2	IGF2BP2	P	P	P	P	2.2	2.8	1.1	1.5
219177_at	Hs.718510	BRX1, biogenesis of ribosomes, homolog (*S. cerevisiae*)	BRIX1	P	P	P	P	1.6	2.8	−1.1	1.6
219735_s_at	Hs.156471	Transcription factor CP2-like 1	TFCP2L1	A	P	P	P	3.5	2.7	1.2	−1.1
219823_at	Hs.86154	Lin-28 homolog (*C. elegans*)	LIN28	A	P	P	P	25980.2	23501.4	1.1	1.0
220053_at	Hs.86232	Growth differentiation factor 3	GDF3	A	P	P	P	15.8	22.7	−1.1	1.3
220184_at	Hs.635882	Nanog homeobox	NANOG	A	P	P	P	15134.8	13855.2	1.4	1.3
220668_s_at	Hs.643024	DNA (cytosine-5-)-methyltransferase 3β	DNMT3B	P	P	P	P	99.7	82.3	1.2	−1.1
221728_x_at	Hs.730656	X (inactive)-specific transcript (nonprotein coding)	XIST	P	P	A	A	−1.3	−88.8	1945.5	27.6
222176_at	Hs.500466	Phosphatase and tensin homolog	PTEN	A	A	A	A	−3.7	−7.5	−3.4	−6.9
223121_s_at	Hs.481022	Secreted frizzled-related protein 2	SFRP2	A	P	P	P	258.7	375.6	−1.1	1.3
223122_s_at	Hs.481022	Secreted frizzled-related protein 2	SFRP2	A	P	P	P	1264.8	14.76.7	−1.4	−1.2
223963_s_at	Hs.35354	Insulin-like growth factor 2 mRNA binding protein 2	IGF2BP2	P	M	P	A	1.3	1.4	−1.2	−1.1
224588_at	Hs.730656	X (inactive)-specific transcript (nonprotein coding)	XIST	P	P	A	A	−1.3	−176.7	355.0	2.7
224589_at	Hs.730656	X (inactive)-specific transcript (nonprotein coding)	XIST	P	P	A	A	−2.5	−187.9	7.8	−9.6
224590_at	Hs.730656	X (inactive)-specific transcript (nonprotein coding)	XIST	P	P	A	A	−5.7	−128.8	34.4	1.5
225363_at	Hs.500466	Phosphatase and tensin homolog	PTEN	P	P	P	P	−1.9	−3.0	1.1	−1.4
225571_at	Hs.133421	Leukemia inhibitory factor receptor α	LIFR	P	P	P	P	14.0	14.3	1.3	1.3
225575_at	Hs.133421	Leukemia inhibitory factor receptor α	LIFR	P	P	P	P	6.4	6.5	1.4	1.4
227642_at	Hs.156471	Transcription factor CP2-like 1	TFCP2L1	A	P	P	P	29.3	33.4	1.4	1.6
227671_at	Hs.730656	X (inactive)-specific transcript (nonprotein coding)	XIST	P	P	A	A	−1.0	−66.6	44.9	−1.4
227690_at	Hs.302352	γ-Aminobutyric acid (GABA) A receptor, β3	GABRB3	A	P	P	P	133.3	161.2	1.0	1.2
227771_at	Hs.133421	Leukemia inhibitory factor receptor α	LIFR	P	P	P	P	2.9	1.8	1.1	−1.5
227830_at	Hs.302352	γ-Aminobutyric acid (GABA) A receptor, β3	GABRB3	A	P	P	P	121.6	129.7	1.2	1.2
228038_at	Hs.518438	SRY (sex-determining region Y)-box 2	SOX2	A	P	P	P	8739.3	7576.9	1.2	1.1
229282_at	Hs.514746	GATA binding protein 6	GATA6	M	M	P	A	1.7	1.6	3.1	3.0
229341_at	Hs.156471	Transcription factor CP2-like 1	TFCP2L1	A	A	A	A	1.2	2.9	−3.9	−1.6

(*continued*)

Table 3. Gene Expression Data of the Probe Sets in the Affymetrix Human Genome U133 Plus 2.0 Array for the Characterization of Undifferentiated Stem Cells (*Continued*)

				Flag[a]				Fold Change Versus DMC54		Fold Change Versus KhES1	
Probe Set ID	UniGene ID	Gene Title	Symbol	DMC54	DMC5403	DMC5413	KhES1	DMC5403	DMC5413	DMC5403	DMC5413
229724_at	Hs.302352	γ-Aminobutyric acid (GABA) A receptor, β3	GABRB3	A	P	P	P	51.7	53.0	1.2	1.3
230462_at	Hs.654609	Numb homolog (Drosophila)	NUMB	P	P	P	P	2.1	1.6	−1.4	−1.9
230916_at	Hs.370414	Nodal homolog (mouse)	NODAL	A	P	P	P	26.2	27.7	1.0	1.1
231798_at	Hs.248201	Noggin	NOG	P	P	P	P	−17.0	−13.5	1.2	1.5
233254_x_at	Hs.500466	Phosphatase and tensin homolog	PTEN	A	A	A	A	1.1	−1.6	−1.1	−2.0
233314_at	Hs.500466	Phosphatase and tensin homolog	PTEN	A	P	A	P	17.2	2.4	1.0	−7.2
233317_at	Hs.114286	CD9 molecule	CD9	A	A	A	A	8.2	1.9	1.4	−3.0
233322_at	Hs.114286	CD9 molecule	CD9	A	A	A	A	2.1	1.9	5.7	5.0
234474_x_at	Hs.532082	Interleukin 6 signal transducer (gp130, oncostatin M receptor)	IL6ST	A	A	A	A	−9.9	−15.9	−1.8	−2.9
234967_at	Hs.532082	Interleukin 6 signal transducer (gp130, oncostatin M receptor)	IL6ST	A	A	A	A	−2.8	−3.0	−4.4	−4.8
235446_at	Hs.724376	X (inactive)-specific transcript (nonprotein coding)	XIST	A	A	A	A	1.5	−1.1	1.2	−1.4
236930_at	Hs.654609	Numb homolog (Drosophila)	NUMB	A	P	P	P	2.3	2.1	−1.6	−1.7
237896_at	Hs.370414	Nodal homolog (mouse)	NODAL	A	P	P	P	6.3	5.6	1.1	−1.0
241609_at	Hs.546573	Forkhead box D3	FOXD3	A	A	A	A	2.9	7.7	2.0	5.3
241612_at	Hs.546573	Forkhead box D3	FOXD3	A	P	P	P	758.4	868.1	1.0	1.2
242622_x_at	Hs.500466	Phosphatase and tensin homolog	PTEN	A	A	A	A	1.2	−1.1	−2.6	−3.6
243161_x_at	Hs.335787	Zinc finger protein 42 homolog (mouse)	ZFP42	A	P	P	P	8492.4	8389.2	−1.3	−1.3
243712_at	Hs.730656	X (inactive)-specific transcript (nonprotein coding)	XIST	A	A	A	A	1.3	1.9	−1.8	−1.2
244163_at	Hs.252451	Sema domain, immunoglobulin domain (Ig), short basic domain, secreted, (semaphorin) 3A	SEMA3A	P	P	P	P	1.2	−1.2	1.7	1.2
244849_at	Hs.252451	Sema domain, immunoglobulin domain (Ig), short basic domain, secreted, (semaphorin) 3A	SEMA3A	P	P	A	P	1.8	−1.4	1.3	−1.9

[a]Flag indicates whether a transcript is present (P), marginal (M), or absent (A), as assigned by the Detection Algorithm.

or fewer factors, that is, c-MYC is not required (30). Although we tried several times to reprogram the DMCs using OSK, we could not generate hiPSCs (unpublished results). The lower endogenous expression of MYCL1 in the DMCs compared with DFBs might explain the reduced efficiency of DMC reprogramming when c-MYC is omitted.

We also evaluated the expression of the GLIS1 homologs GLIS2 and GLIS3 in several cell lines and tissues (Fig. 8). GLIS2 and GLIS3 were hardly expressed in pluripotent stem cells (hESCs and hiPSCs), placenta, or testis (Fig. 8). In contrast, placenta-derived cells (AECs, AMCs, DMCs), BM-MSCs, and DFBs expressed GLIS2 and GLIS3; in particular, DFBs highly expressed both GLIS1 homologs (Fig. 8). Although the significance of GLIS2 and GLIS3 in generating hiPSCs is not yet clear, these differences in GLI-related Krüppel-like zinc finger genes might result in different efficiencies of hiPSC generation from various cell sources. Another factor, Zscan4, was previously shown to facilitate the reprogramming of MEFs (12). Unlike in MEFs, we detected an increase in the intrinsic expression of ZSCAN4 in human DMCs and DFBs when the reprogramming factors were overexpressed; however, ZSCAN4's contribution to iPSC generation has yet to be elucidated. Zscan4 was shown to be required only for the first few days of iPSC formation and to mediate the activation of genes detected only in preimplantation embryos (1-cell to blastocyst) (12). Besides

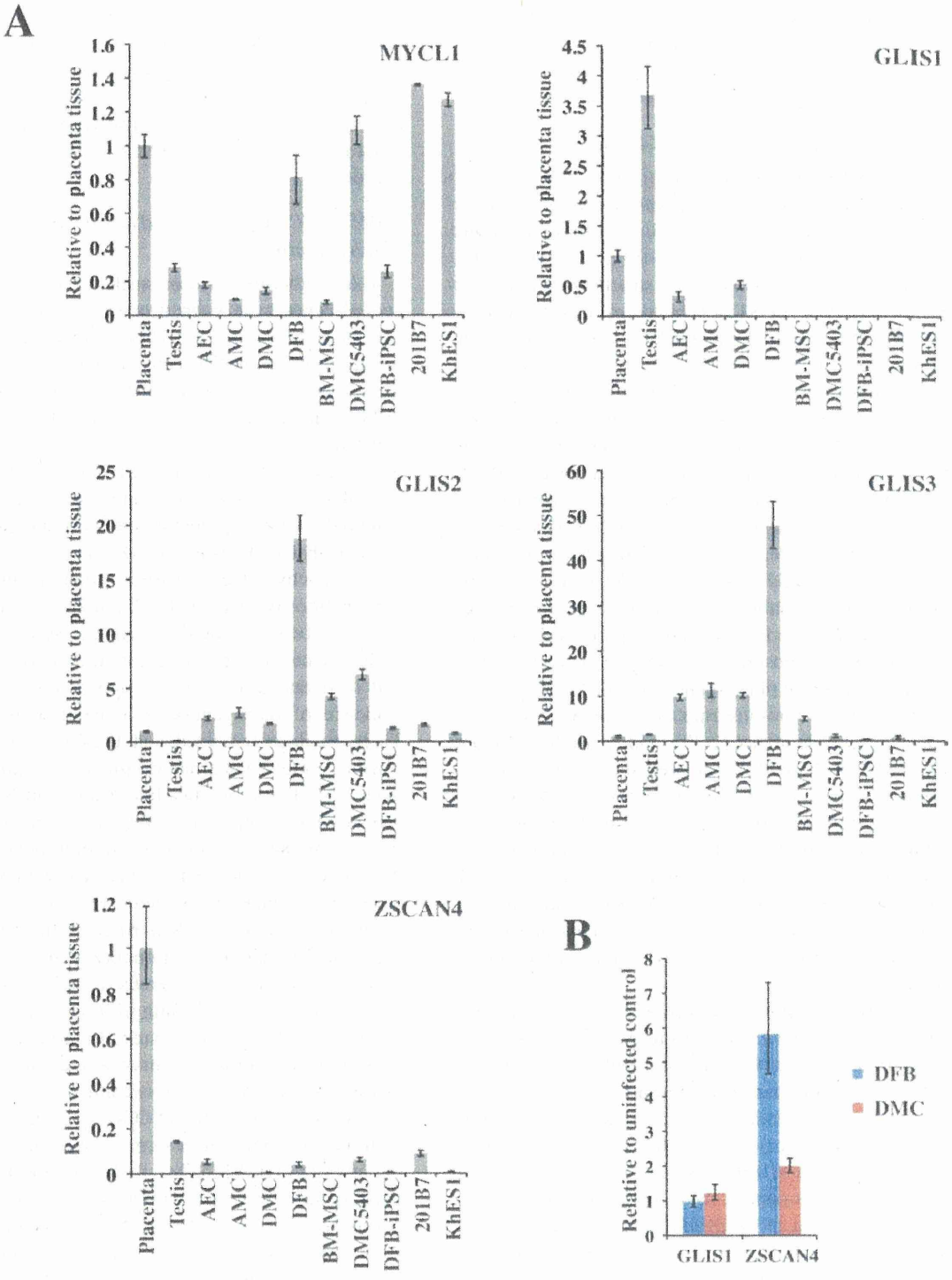

Figure 8. Transcriptional expression of novel factors for efficient reprogramming. (A) Endogenous transcriptional expression of MYCL1 (top left), GLIS1 (top right), GLIS2 (middle left), GLIS3 (middle right), and ZSCAN4 (bottom left). GAPDH was used as the internal control gene, and data are presented relative to the values from placenta tissue and as the mean ± SD ($n = 3$). (B) Expression of GLIS1 and ZSCAN4 3 days after the transduction of reprogramming factor genes. Results are shown in comparison to individual uninfected control cells. See Table 1 for gene definitions.

GLIS1 and ZSCAN4, other preimplantation-specific genes that are expressed in blastomeres and have reprogramming activity in nuclear transplantation (5) should be considered for improving the generation of iPSCs.

Molecular Characteristics of DMC-hiPSCs

The global expression profile of DMC-iPSC clones, which retained a hESC-like morphology after several passages, verified that there was a strong similarity between DMC-hiPSCs and KhES1 ($p>0.98$) (Fig. 7A). Despite the similarities, one of the genes for characterizing undifferentiated ES cells (2), XIST, was highly expressed in one of the DMC-iPSC clones (DMC5403), that is, at more than 10 times the level in female hESCs (KhES1), and at the same level as in the parental DMCs. In female cells, one of the two X-chromosomes is transcriptionally silenced through a process called X-chromosome inactivation (XCI); this process depends on the large noncoding RNA XIST (45). In the mouse system, the key pluripotency factors Nanog, Oct3/4, and Sox2 bind within Xist's intron 1 and cooperate to repress the Xist transcript in undifferentiated embryonic stem (ES) cells; therefore, both X-chromosomes remain active (Xa) (32). In the process of reprogramming female somatic cells to miPSCs, the inactivated X-chromosome (Xi) is reactivated in concert with the activation of pluripotency factors (25,40). On the other hand, the X-chromosomes of female hESCs have a variable epigenetic status (2,39), and many hESC lines display XCI in the undifferentiated state. Studies of the epigenetic state of the X-chromosomes in hiPSCs have led to two conflicting conclusions. One study showed that a hiPSC clone, unlike miPSCs, was reprogrammed without undergoing X-reactivation and maintained the XCI of the mother fibroblast cell (44). Another study showed that complete X-reactivation was achieved in some hiPSC lines and that subsequent X-inactivation occurred during differentiation (26).

We briefly examined the epigenetic state by assessing the XIST expression and performing MSP analysis of the XIST promoter region. In agreement with the expectation that XIST would be silenced on Xa and actively expressed from Xi, the results indicated that Xi/Xa was present in the parental female cells and in the early phase of one DMC-hiPSC clone (DMC5403 at passage 5). In contrast, Xa/Xa was present in the other DMC-hiPSC clone (DMC5413) and in DFB-hiPSCs (Fig. 7B). DMC5403 cells from multiply passaged cultures did not express the XIST gene, although the XIST promoter region in half of the chromosomes remained unmethylated. The silencing of XIST expression in the presence of an inactive X is often observed in both undifferentiated and differentiated cell states (39,44). Overall, regardless of the epigenetic state of the X-chromosome, the DMC-iPSC clones exhibited genome-wide expression profiles similar to those of hESCs and formed differentiated tissues containing all three germ layers in vitro and in vivo (early passage, Figs. 5–7) (late passage, data not shown). Thus, not just the X-chromosome but the overall epigenetic state of iPSCs is an important quality and safety concern in clinical applications of hiPSCs and remains to be fully addressed.

DMC-hiPSCs May Be Useful as Allogeneic hiPSCs in Regenerative Medicine

Extraembryonic tissues such as the umbilical cord and placenta have been proposed as attractive human cell sources for use in regenerative medicine. In addition, human amnion-derived cells, which are of fetal origin, were reported as a promising cell source for efficient hiPSC generation (4,29,48). In this study, we used DMCs isolated from the decidua membrane, which is a maternal portion of the placenta (18). DMCs exhibit a typical fibroblast-like morphology and have a high proliferative potential for over 30 population doublings, which is better than that of BM-MSCs (18). They strongly express the mesenchymal cell marker vimentin, but not cytokeratin 19 or HLA-G, and FCM analysis shows a resemblance between DMCs and BM-MSCs. In vitro, the DMCs showed good differentiation into chondrocytes and moderate differentiation into adipocytes, but scant evidence of osteogenesis, compared with BM-MSCs. These findings indicated that DMCs are mesenchymal cells of purely maternal origin and unique cells that have MSC-like properties but differ from BM-MSCs. It was previously reported that mesenchymal cells derived from the human term decidua are multipotent, and these decidua-derived mesenchymal cells were suggested to be useful for regenerative medicine (11,13,23). However, in the mouse system, MSCs purified from adult tissue are useful for producing high-quality iPSCs (33). In addition, iPSCs have been generated efficiently from various somatic stem cells, including MSCs (4,33,35) and neural stem cells (6,19). In this context, the generation of iPSCs from immature somatic stem cells is an important option that needs to be thoroughly examined.

Here, we showed that DMCs can be efficiently reprogrammed into pluripotent stem cells. Although DMCs are not superior to BM-MSCs in their multipotency and might have some risk of genomic abnormalities accumulated during aging, their greater proliferative ability means that their cultivation might require less maintenance, and their derivation from the maternal portion of the human fetal adnexal tissues, which are otherwise discarded, would resolve many ethical concerns associated with the use of embryonic stem cells. The high success rate of DMC isolation from tissues stored more than 24 h indicates that it may be feasible to develop a system for collecting and banking fetal adnexal tissues; such a bank would provide

tissues of wide HLA variation to multiple and even remote hospitals (18). We also previously reported that the pericellular matrix prepared from DMCs (PCM-DM) is as potent a substrate for the growth and pluripotency of hESCs as Matrigel (28). Furthermore, we have confirmed that hiPSCs can be generated on PCM-DM by a retroviral gene transduction procedure (Fukusumi et al., submitted).

To be sure, many concerns about the feasibility and potential risks of cell-based therapies using iPSCs have been recognized, and many scientific and technical issues remain to be elucidated before iPSC technology can be applied to regenerative medicine. Since patient safety is the foremost consideration, extensive exploration and testing of iPSCs will be required before this technology can be considered for clinical use.

Taken together, these findings indicate that DMCs have several advantages for clinical use and that the generation of hiPSCs from DMCs might enable the establishment of hiPSC-banking systems. Such systems could increase the availability of allogeneic hiPSCs that have broad HLA variations and thus increase the feasibility of their use in clinical applications.

ACKNOWLEDGMENTS: We thank Dr. Chiaki Ban (Department of Obstetrics and Gynecology Osaka National Hospital) and Ms. Chika Teramoto and Ms. Ai Takada (Osaka National Hospital) for support in collecting the human placenta tissues. We also thank Mr. Kenji Kawai and Ms. Miyuki Kuromuma (CIEA) for support in the teratoma formation assay. This study was supported by the Project for the Realization of Regenerative Medicine, the Ministry of Education, Culture, Sports, Science and Technology (MEXT) of Japan, the Cooperative Link of Unique Science and Technology for Economy Revitalization (CLUSTER) project from MEXT, Japan, and the Research on New Drug Development, Health and Labour Sciences Research Grants, the Ministry of Health, Labour and Welfare (MHLW) of Japan. The authors declare no conflicts of interest.

REFERENCES

1. Aasen, T.; Raya, A.; Barrero, M. J.; Garreta, E.; Consiglio, A.; Gonzalez, F.; Vassena, R.; Bilic, J.; Pekarik, V.; Tiscornia, G.; Edel, M.; Boue, S.; Izpisua Belmonte, J. C. Efficient and rapid generation of induced pluripotent stem cells from human keratinocytes. Nat. Biotechnol. 26(11):1276–1284; 2008.
2. Adewumi, O.; Aflatoonian, B.; Ahrlund-Richter, L.; Amit, M.; Andrews, P. W.; Beighton, G.; Bello, P. A.; Benvenisty, N.; Berry, L. S.; Bevan, S.; Blum, B.; Brooking, J.; Chen, K. G.; Choo, A. B. H.; Churchill, G. A.; Corbel, M.; Damjanov, I.; Draper, J. S.; Dvorak, P.; Emanuelsson, K.; Fleck, R. A.; Ford, A.; Gertow, K.; Gertsenstein, M.; Gokhale, P. J.; Hamilton, R. S.; Hampl, A.; Healy, L. E.; Hovatta, O.; Hyllner, J.; Imreh, M. P.; Itskovitz-Eldor, J.; Jackson, J.; Johnson, J. L.; Jones, M.; Kee, K.; King, B. L.; Knowles, B. B.; Lako, M.; Lebrin, F.; Mallon, B. S.; Manning, D.; Mayshar, Y.; McKay, R. D. G.; Michalska, A. E.; Mikkola, M.; Mileikovsky, M.; Minger, S. L.; Moore, H. D.; Mummery, C. L.; Nagy, A.; Nakatsuji, N.; O'Brien, C. M.; Oh, S. K. W.; Olsson, C.; Otonkoski, T.; Park, K.-Y.; Passier, R.; Patel, H.; Patel, M.; Pedersen, R.; Pera, M. F.; Piekarczyk, M. S.; Pera, R. A. R.; Reubinoff, B. E.; Robins, A. J.; Rossant, J.; Rugg-Gunn, P.; Schulz, T. C.; Semb, H.; Sherrer, E. S.; Siemen, H.; Stacey, G. N.; Stojkovic, M.; Suemori, H.; Szatkiewicz, J.; Turetsky, T.; Tuuri, T.; van den Brink, S.; Vintersten, K.; Vuoristo, S.; Ward, D.; Weaver, T. A.; Young, L. A.; Zhang, W. Characterization of human embryonic stem cell lines by the International Stem Cell Initiative. Nat. Biotechnol. 25(7):803–816; 2007.
3. Barlow, S.; Brooke, G.; Chatterjee, K.; Price, G.; Pelekanos, R.; Rossetti, T.; Doody, M.; Venter, D.; Pain, S.; Gilshenan, K.; Atkinson, K. Comparison of human placenta- and bone marrow-derived multipotent mesenchymal stem cells. Stem Cells Dev. 17:1095–1107; 2008.
4. Cai, J.; Li, W.; Su, H.; Qin, D.; Yang, J.; Zhu, F.; Xu, J.; He, W.; Guo, X.; Labuda, K.; Peterbauer, A.; Wolbank, S.; Zhong, M.; Li, Z.; Wu, W.; So, K. F.; Redl, H.; Zeng, L.; Esteban, M. A.; Pei, D. Generation of human induced pluripotent stem cells from umbilical cord matrix and amniotic membrane mesenchymal cells. J. Biol. Chem. 285:11227–11234; 2010.
5. Egli, D.; Sandler, V. M.; Shinohara, M. L.; Cantor, H.; Eggan, K. Reprogramming after chromosome transfer into mouse blastomeres. Curr. Biol. 19:1403–1409; 2009.
6. Eminli, S.; Utikal, J.; Arnold, K.; Jaenisch, R.; Hochedlinger, K. Reprogramming of neural progenitor cells into induced pluripotent stem cells in the absence of exogenous Sox2 expression. Stem Cells 26:2467–2474; 2008.
7. Falco, G.; Lee, S. L.; Stanghellini, I.; Bassey, U. C.; Hamatani, T.; Ko, M. S. Zscan4: A novel gene expressed exclusively in late 2-cell embryos and embryonic stem cells. Dev. Biol. 307:539–550; 2007.
8. Fukuchi, Y.; Nakajima, H.; Sugiyama, D.; Hirose, I.; Kitamura, T.; Tsuji, K. Human placenta-derived cells have mesenchymal stem/progenitor cell potential. Stem Cells 22:649–658; 2004.
9. Haase, A.; Olmer, R.; Schwanke, K.; Wunderlich, S.; Merkert, S.; Hess, C.; Zweigerdt, R.; Gruh, I.; Meyer, J.; Wagner, S.; Maier, L. S.; Han, D. W.; Glage, S.; Miller, K.; Fischer, P.; Scholer, H. R.; Martin, U. Generation of induced pluripotent stem cells from human cord blood. Cell Stem Cell 5:434–441; 2009.
10. Hanna, J.; Markoulaki, S.; Schorderet, P.; Carey, B. W.; Beard, C.; Wernig, M.; Creyghton, M. P.; Steine, E. J.; Cassady, J. P.; Foreman, R.; Lengner, C. J.; Dausman, J. A.; Jaenisch, R. Direct reprogramming of terminally differentiated mature B lymphocytes to pluripotency. Cell 133:250–264; 2008.
11. Hayati, A. R.; Nur Fariha, M. M.; Tan, G. C.; Tan, A. E.; Chua, K. Potential of human decidua stem cells for angiogenesis and neurogenesis. Arch. Med. Res. 42:291–300; 2011.
12. Hirata, T.; Amano, T.; Nakatake, Y.; Amano, M.; Piao, Y.; Hoang, H. G.; Ko, M. S. Zscan4 transiently reactivates early embryonic genes during the generation of induced pluripotent stem cells. Sci. Rep. 2:208; 2012.
13. Huang, Y. C.; Yang, Z. M.; Chen, X. H.; Tan, M. Y.; Wang, J.; Li, X. Q.; Xie, H. Q.; Deng, L. Isolation of mesenchymal stem cells from human placental decidua basalis and resistance to hypoxia and serum deprivation. Stem Cell Rev. 5:247–255; 2009.
14. Igura, K.; Zhang, X.; Takahashi, K.; Mitsuru, A.; Yamaguchi, S.; Takashi, T. A. Isolation and characterization of mesenchymal progenitor cells from chorionic villi of human placenta. Cytotherapy 6:543–553; 2004.

15. In 't Anker, P. S.; Scherjon, S. A.; Kleijburg-van der Keur, C.; de Groot-Swings, G. M.; Claas, F. H.; Fibbe, W. E.; Kanhai, H. H. Isolation of mesenchymal stem cells of fetal or maternal origin from human placenta. Stem Cells 22:1338–1345; 2004.
16. Ito, M.; Hiramatsu, H.; Kobayashi, K.; Suzue, K.; Kawahata, M.; Hioki, K.; Ueyama, Y.; Koyanagi, Y.; Sugamura, K.; Tsuji, K.; Heike, T.; Nakahata, T. NOD/SCID/gamma(c) (null) mouse: An excellent recipient mouse model for engraftment of human cells. Blood 100:3175–3182; 2002.
17. Izumi, M.; Pazin, B. J.; Minervini, C. F.; Gerlach, J.; Ross, M. A.; Stolz, D. B.; Turner, M. E.; Thompson, R. L.; Miki, T. Quantitative comparison of stem cell marker-positive cells in fetal and term human amnion. J. Reprod. Immunol. 81:39–43; 2009.
18. Kanematsu, D.; Shofuda, T.; Yamamoto, A.; Ban, C.; Ueda, T.; Yamasaki, M.; Kanemura, Y. Isolation and cellular properties of mesenchymal cells derived from the decidua of human term placenta. Differentiation 82:77–88; 2011.
19. Kim, J. B.; Sebastiano, V.; Wu, G.; Arauzo-Bravo, M. J.; Sasse, P.; Gentile, L.; Ko, K.; Ruau, D.; Ehrich, M.; van den Boom, D.; Meyer, J.; Hubner, K.; Bernemann, C.; Ortmeier, C.; Zenke, M.; Fleischmann, B. K.; Zaehres, H.; Scholer, H. R. Oct4-induced pluripotency in adult neural stem cells. Cell 136:411–419; 2009.
20. Livak, K. J.; Schmittgen, T. D. Analysis of relative gene expression data using real-time quantitative PCR and the 2(-Delta Delta C(T)) Method. Methods 25:402–408; 2001.
21. Loh, Y. H.; Agarwal, S.; Park, I. H.; Urbach, A.; Huo, H.; Heffner, G. C.; Kim, K.; Miller, J. D.; Ng, K.; Daley, G. Q. Generation of induced pluripotent stem cells from human blood. Blood 113:5476–5479; 2009.
22. Lowry, W. E.; Richter, L.; Yachechko, R.; Pyle, A. D.; Tchieu, J.; Sridharan, R.; Clark, A. T.; Plath, K. Generation of human induced pluripotent stem cells from dermal fibroblasts. Proc. Natl. Acad. Sci. USA 105:2883–2888; 2008.
23. Macias, M. I.; Grande, J.; Moreno, A.; Dominguez, I.; Bornstein, R.; Flores, A. I. Isolation and characterization of true mesenchymal stem cells derived from human term decidua capable of multilineage differentiation into all 3 embryonic layers. Am. J. Obstet. Gynecol. 203:e495; 2010.
24. Maekawa, M.; Yamaguchi, K.; Nakamura, T.; Shibukawa, R.; Kodanaka, I.; Ichisaka, T.; Kawamura, Y.; Mochizuki, H.; Goshima, N.; Yamanaka, S. Direct reprogramming of somatic cells is promoted by maternal transcription factor Glis1. Nature 474:225–229; 2011.
25. Maherali, N.; Sridharan, R.; Xie, W.; Utikal, J.; Eminli, S.; Arnold, K.; Stadtfeld, M.; Yachechko, R.; Tchieu, J.; Jaenisch, R.; Plath, K.; Hochedlinger, K. Directly reprogrammed fibroblasts show global epigenetic remodeling and widespread tissue contribution. Cell Stem Cell 1:55–70; 2007.
26. Marchetto, M. C. N.; Carromeu, C.; Acab, A.; Yu, D.; Yeo, G. W.; Mu, Y.; Chen, G.; Gage, F. H.; Muotri, A. R. A Model for neural development and treatment of rett syndrome using human induced pluripotent stem cells. Cell 143:527–539; 2010.
27. Meissner, A.; Wernig, M.; Jaenisch, R. Direct reprogramming of genetically unmodified fibroblasts into pluripotent stem cells. Nat. Biotechnol. 25:1177–1181; 2007.
28. Nagase, T.; Ueno, M.; Matsumura, M.; Muguruma, K.; Ohgushi, M.; Kondo, N.; Kanematsu, D.; Kanemura, Y.; Sasai, Y. Pericellular matrix of decidua-derived mesenchymal cells: A potent human-derived substrate for the maintenance culture of human ES cells. Dev. Dyn. 238: 1118–1130; 2009.
29. Nagata, S.; Toyoda, M.; Yamaguchi, S.; Hirano, K.; Makino, H.; Nishino, K.; Miyagawa, Y.; Okita, H.; Kiyokawa, N.; Nakagawa, M.; Yamanaka, S.; Akutsu, H.; Umezawa, A.; Tada, T. Efficient reprogramming of human and mouse primary extraembryonic cells to pluripotent stem cells. Genes Cells 14:1395–1404; 2009.
30. Nakagawa, M.; Koyanagi, M.; Tanabe, K.; Takahashi, K.; Ichisaka, T.; Aoi, T.; Okita, K.; Mochiduki, Y.; Takizawa, N.; Yamanaka, S. Generation of induced pluripotent stem cells without Myc from mouse and human fibroblasts. Nat. Biotechnol. 26:101–106; 2008.
31. Nakagawa, M.; Takizawa, N.; Narita, M.; Ichisaka, T.; Yamanaka, S. Promotion of direct reprogramming by transformation-deficient Myc. Proc. Natl. Acad. Sci. USA 107:14152–14157; 2010.
32. Navarro, P.; Chambers, I.; Karwacki-Neisius, V.; Chureau, C.; Morey, C.; Rougeulle, C.; Avner, P. Molecular coupling of xist regulation and pluripotency. Science 321:1693–1695; 2008.
33. Niibe, K.; Kawamura, Y.; Araki, D.; Morikawa, S.; Miura, K.; Suzuki, S.; Shimmura, S.; Sunabori, T.; Mabuchi, Y.; Nagai, Y.; Nakagawa, T.; Okano, H.; Matsuzaki, Y. Purified mesenchymal stem cells are an efficient source for iPS cell induction. PLoS One 6:e17610; 2011.
34. Nori, S.; Okada, Y.; Yasuda, A.; Tsuji, O.; Takahashi, Y.; Kobayashi, Y.; Fujiyoshi, K.; Koike, M.; Uchiyama, Y.; Ikeda, E.; Toyama, Y.; Yamanaka, S.; Nakamura, M.; Okano, H. Grafted human-induced pluripotent stem cell-derived neurospheres promote motor functional recovery after spinal cord injury in mice. Proc. Nat. Acad. Sci. USA 108:16825–16830; 2011.
35. Oda, Y.; Yoshimura, Y.; Ohnishi, H.; Tadokoro, M.; Katsube, Y.; Sasao, M.; Kubo, Y.; Hattori, K.; Saito, S.; Horimoto, K.; Yuba, S.; Ohgushi, H. Induction of pluripotent stem cells from human third molar mesenchymal stromal cells. J. Biol. Chem. 285:29270–29278; 2010.
36. Okita, K.; Matsumura, Y.; Sato, Y.; Okada, A.; Morizane, A.; Okamoto, S.; Hong, H.; Nakagawa, M.; Tanabe, K.; Tezuka, K.-i.; Shibata, T.; Kunisada, T.; Takahashi, M.; Takahashi, J.; Saji, H.; Yamanaka, S. A more efficient method to generate integration-free human iPS cells. Nat. Methods 8:409–412; 2011.
37. Park, I. H.; Zhao, R.; West, J. A.; Yabuuchi, A.; Huo, H.; Ince, T. A.; Lerou, P. H.; Lensch, M. W.; Daley, G. Q. Reprogramming of human somatic cells to pluripotency with defined factors. Nature 451:141–146; 2008.
38. Silva, J.; Nichols, J.; Theunissen, T. W.; Guo, G.; van Oosten, A. L.; Barrandon, O.; Wray, J.; Yamanaka, S.; Chambers, I.; Smith, A. Nanog is the gateway to the pluripotent ground state. Cell 138:722–737; 2009.
39. Silva, S. S.; Rowntree, R. K.; Mekhoubad, S.; Lee, J. T. X-chromosome inactivation and epigenetic fluidity in human embryonic stem cells. Proc. Nat. Acad. Sci. USA 105:4820–4825; 2008.
40. Stadtfeld, M.; Maherali, N.; Breault, D. T.; Hochedlinger, K. Defining molecular cornerstones during fibroblast to iPS cell reprogramming in mouse. Cell Stem Cell 2:230–240; 2008.

41. Suemori, H.; Yasuchika, K.; Hasegawa, K.; Fujioka, T.; Tsuneyoshi, N.; Nakatsuji, N. Efficient establishment of human embryonic stem cell lines and long-term maintenance with stable karyotype by enzymatic bulk passage. Biochem. Biophys. Res. Commun. 345:926–932; 2006.
42. Takahashi, K.; Tanabe, K.; Ohnuki, M.; Narita, M.; Ichisaka, T.; Tomoda, K.; Yamanaka, S. Induction of pluripotent stem cells from adult human fibroblasts by defined factors. Cell 131:861–872; 2007.
43. Takahashi, K.; Yamanaka, S. Induction of pluripotent stem cells from mouse embryonic and adult fibroblast cultures by defined factors. Cell 126:663–676; 2006.
44. Tchieu, J.; Kuoy, E.; Chin, M. H.; Trinh, H.; Patterson, M.; Sherman, S. P.; Aimiuwu, O.; Lindgren, A.; Hakimian, S.; Zack, J. A.; Clark, A. T.; Pyle, A. D.; Lowry, W. E.; Plath, K. Female human iPSCs retain an inactive X chromosome. Cell Stem Cell 7:329–342; 2010.
45. Wutz, A.; Jaenisch, R. A shift from reversible to irreversible X inactivation is triggered during ES cell differentiation. Mol. Cell 5:695–705; 2000.
46. Yen, B. L.; Huang, H. I.; Chien, C. C.; Jui, H. Y.; Ko, B. S.; Yao, M.; Shun, C. T.; Yen, M. L.; Lee, M. C.; Chen, Y. C. Isolation of multipotent cells from human term placenta. Stem Cells 23:3–9; 2005.
47. Yu, J.; Vodyanik, M. A.; Smuga-Otto, K.; Antosiewicz-Bourget, J.; Frane, J. L.; Tian, S.; Nie, J.; Jonsdottir, G. A.; Ruotti, V.; Stewart, R.; Slukvin, I. I.; Thomson, J. A. Induced pluripotent stem cell lines derived from human somatic cells. Science 318:1917–1920; 2007.
48. Zhao, H. X.; Li, Y.; Jin, H. F.; Xie, L.; Liu, C.; Jiang, F.; Luo, Y. N.; Yin, G. W.; Wang, J.; Li, L. S.; Yao, Y. Q.; Wang, X. H. Rapid and efficient reprogramming of human amnion-derived cells into pluripotency by three factors OCT4/SOX2/NANOG. Differentiation 80:123–129; 2010.

OPEN ACCESS Freely available online

PLOS ONE

Protein Kinase C Regulates Human Pluripotent Stem Cell Self-Renewal

Masaki Kinehara[1], Suguru Kawamura[1], Daiki Tateyama[1], Mika Suga[1], Hiroko Matsumura[1], Sumiyo Mimura[1], Noriko Hirayama[2], Mitsuhi Hirata[1], Kozue Uchio-Yamada[3], Arihiro Kohara[2], Kana Yanagihara[1], Miho K. Furue[1]*

1 Laboratory of Stem Cell Cultures, Department of Disease Bioresources Research, National Institute of Biomedical Innovation, Ibaraki, Osaka, Japan, **2** Laboratory of Cell Cultures, Department of Disease Bioresources Research, National Institute of Biomedical Innovation, Ibaraki, Osaka, Japan, **3** Laboratory of Animal Models for Human Diseases, Department of Disease Bioresources Research, National Institute of Biomedical Innovation, Ibaraki, Osaka, Japan

Abstract

Background: The self-renewal of human pluripotent stem (hPS) cells including embryonic stem and induced pluripotent stem cells have been reported to be supported by various signal pathways. Among them, fibroblast growth factor-2 (FGF-2) appears indispensable to maintain self-renewal of hPS cells. However, downstream signaling of FGF-2 has not yet been clearly understood in hPS cells.

Methodology/Principal Findings: In this study, we screened a kinase inhibitor library using a high-throughput alkaline phosphatase (ALP) activity-based assay in a minimal growth factor-defined medium to understand FGF-2-related molecular mechanisms regulating self-renewal of hPS cells. We found that in the presence of FGF-2, an inhibitor of protein kinase C (PKC), GF109203X (GFX), increased ALP activity. GFX inhibited FGF-2-induced phosphorylation of glycogen synthase kinase-3β (GSK-3β), suggesting that FGF-2 induced PKC and then PKC inhibited the activity of GSK-3β. Addition of activin A increased phosphorylation of GSK-3β and extracellular signal-regulated kinase-1/2 (ERK-1/2) synergistically with FGF-2 whereas activin A alone did not. GFX negated differentiation of hPS cells induced by the PKC activator, phorbol 12-myristate 13-acetate whereas Gö6976, a selective inhibitor of PKCα, β, and γ isoforms could not counteract the effect of PMA. Intriguingly, functional gene analysis by RNA interference revealed that the phosphorylation of GSK-3β was reduced by siRNA of PKCδ, PKCε, and ζ, the phosphorylation of ERK-1/2 was reduced by siRNA of PKCε and ζ, and the phosphorylation of AKT was reduced by PKCε in hPS cells.

Conclusions/Significance: Our study suggested complicated cross-talk in hPS cells that FGF-2 induced the phosphorylation of phosphatidylinositol-3 kinase (PI3K)/AKT, mitogen-activated protein kinase/ERK-1/2 kinase (MEK), PKC/ERK-1/2 kinase, and PKC/GSK-3β. Addition of GFX with a MEK inhibitor, U0126, in the presence of FGF-2 and activin A provided a long-term stable undifferentiated state of hPS cells even though hPS cells were dissociated into single cells for passage. This study untangles the cross-talk between molecular mechanisms regulating self-renewal and differentiation of hPS cells.

Citation: Kinehara M, Kawamura S, Tateyama D, Suga M, Matsumura H, et al. (2013) Protein Kinase C Regulates Human Pluripotent Stem Cell Self-Renewal. PLoS ONE 8(1): e54122. doi:10.1371/journal.pone.0054122

Editor: Tadayuki Akagi, Kanazawa University, Japan

Received April 20, 2012; **Accepted** December 10, 2012; **Published** January 21, 2013

Funding: The funders had no role in study design, data collection and analysis, decision to publish, or preparation of the manuscript. This study was supported by grants-in-aid from the Ministry of Health, Labor and Welfare of Japan to M.K.F. and A.K., the Ministry of Education, Culture, Sports, Science and Technology of Japan to M.K.F. and M.K. and the Japan Science and Technology Agency to M.K.F.

Competing Interests: The authors have read the journal's policy and have the following conflicts: One of the authors, (MKF) has declared a financial interest in a company, Cell Science & Technology Institute Corporation (Sendai, Japan) whose product, a basal medium ESF was used in this study. However, the licensing fee is less than $10,000 per year. This does not alter the authors adherence to all the PLOS ONE policies on sharing data and materials.

* E-mail: mkfurue@nibio.go.jp

Introduction

The self-renewal of human pluripotent stem (hPS) cells including embryonic stem (hES) and induced pluripotent stem (hiPS) cells have been reported to be supported by various signal pathways, including transforming growth factor-β/activin A/Nodal [1–3], sphingosine-1-phosphate/platelet derived growth factor (S1P/PDGF) [4], insulin growth factor (IGF)/insulin [5] and fibroblast growth factor-2 (FGF-2) [6–9]. The process of self-renewal appears to be regulated synergistically through the various pathways via growth factor or cytokine supplementation. Among them, FGF-2 signaling appears indispensable to hPS cells [10–12].

FGF family members including FGF-2, bind to FGF receptors (FGFRs) and induce activation of the mitogen-activated protein kinase/extracellular signal-regulated kinase-1/2 (ERK-1/2) kinase (MEK), phosphatidylinositol-3 kinase (PI3K), and phospholipase C-γ (PLC-γ)/protein kinase C (PKC) pathways [13]. MEK-1/2 activation by FGFR results in ERK-1/2 phosphorylation, which subsequently translocates into the nucleus leading to phosphorylation of transcription factors such as c-Myc, c-Jun, and c-Fos. PI3K, a lipid kinase activates pleckstrin homology (PH) domain containing proteins such as AKT, and 3-phosphoinositide-dependent kinase-1 (PDK1). AKT directly activates murine double minute 2 (MDM2), a negative regulator of p53. p53 is

responsible for DNA damage surveillance and in response initiates cell cycle arrest and DNA repair. Interestingly, AKT also inhibits glycogen synthase kinase-3 (GSK-3), a negative regulator of Wnt signaling by phosphorylation [14]. However, the contributions of FGF-2 downstream pathways in the self-renewal of hPS cells have been controversial [9,14–18]. The ERK pathway has been thought to promote cell proliferation and adhesion but also differentiation in hES cells. The PI3K pathway plays important roles in proliferation, differentiation, survival, and cellular transformation.

Previously, we found that a proteoglycan, heparin promotes FGF-2 activity on the growth of undifferentiated hES cells in a minimal growth factor-defined culture medium, hESF9 [8], in which the effect of exogenous factors can be analyzed without the confounding influences of undefined components [8,19–23] because insulin, transferrin, albumin conjugated with oleic acid, and FGF-2 (10 ng/ml) are the only protein components. Understanding cell signaling in undifferentiated hPS cells has lead to the development of optimal conditions for culturing hPS cells. However, manipulation of hPS cells still remains difficult because hPS cells as a single cell are unstable of self-renewal. Although Rho-associated kinase (ROCK) inhibitor (Y-27632) is quite effective to markedly diminish dissociation-induced apoptosis of single cells of hPS cells [24], the continuous use of the ROCK inhibitor increases differentiated cells [25]. For developing application using hPS cells, such as cell based therapy or toxicity screening tests, handling cell numbers would be beneficial. Even for basic research, handling cell numbers would be useful when the cells are dissociated for passages or differentiation. Presumably, if the culture conditions were able to fully support undifferentiated state, even single cells might maintain undifferentiated state. We suspected that there were unrevealed mechanisms to maintain undifferentiated state of single hPS cells. To further understand FGF-2 related molecular mechanisms regulating self-renewal would enhance understanding unclarified cell signaling in hPS cells. Therefore, we screened a kinase inhibitor library using a high-throughput alkaline phosphatase (ALP) activity-based assay in a minimal growth factor-defined culture medium, hESF9. We found that in the presence of FGF-2, an inhibitor of PKCs, GF109203X (GFX), increased ALP activity, suggesting that PKC reduces self-renewal of hPS cells. GFX inhibited FGF-2-induced GSK-3β phosphorylation. Addition of activin A increased phosphorylation of GSK-3β and ERK-1/2 synergistically with FGF-2 whereas activin A alone did not induce phosphorylation of GSK-3β. GFX negated differentiation of hPS cells induced by a PKC activator, phorbol 12-myristate 13-acetate (PMA) whereas Gö6976, a selective inhibitor of PKCα, β, and γ isoforms did not counteract the effect of PMA. Functional gene analysis by RNA interference revealed that siRNA of PKCδ, ε, and ζ isoforms decreased phosphorylation of GSK-3β and also siRNA of PKCε and ζ isoforms decreased phosphorylation of ERK-1/2 in hPS cells. siRNA of PKCε decreased phosphorylation of AKT. On the basis of these results, we suggest that PKCδ, ε and ζ isoforms are FGF-2 downstream effectors, and they play various roles in regulating hPS cell self-renewal. This study helps to untangle the cross-talk between molecular mechanisms regulating self-renewal and differentiation of hPS cells.

Results

PKC inhibitor increased ALP activity of hiPS cells

Previously, we detected the cell proliferative effect of heparin on hES cells without feeder cells in a minimal growth factor-defined culture medium, hESF9 [8], in which the effect of exogenous factors can be analyzed without the confounding influences of undefined components [8,19–23]. In this culture condition using hESF9 medium (Table S1) on bovine fibronectin (FN), a high-throughput ALP activity-based assay was performed to evaluate a library of chemical kinase inhibitors to understand FGF-2 related molecular mechanisms regulating self-renewal of hPS cells. Nine compounds were found to increase ALP activity of the hiPS cell line 201B7 [26] (Fig. 1): Kenpaullone, which is a substitute for a reprogramming factor KLF-4 in mouse iPS cells [27]; Y-27632, which is a Rho-kinase (ROCK) inhibitor known to enhance hES cells survival [24]; HA-1004, H-89, and HA-1077, which are kinase inhibitors presumed to target ROCK [28]; GF109203X (GFX) [29], which is a inhibitor for PKC isoforms; and H-7, H-8, and H-9, which are also thought to target PKC [30]. These results suggest that FGF-2 induces PKC, and PKC acts downstream of FGF-2 to regulate self-renewal of hPS cells.

Effect of PKC inhibitor on FGF-2 signaling in hPS cells

To examine how GFX influenced FGF-2 signaling in hPS cells, the phosphorylation of AKT, ERK-1/2, and GSK-3β induced by FGF-2 with GFX was confirmed by western blotting analysis (Fig. S1A, S1B, S1C, S1D). Then, the phosphorylation levels were quantified by AlphaScreen® SureFire® assay kit. Human ES cells H9 [31] after starvation of FGF-2 and insulin were treated with FGF-2 with and without GFX. FGF-2 significantly stimulated the phosphorylation of AKT, ERK-1/2, and GSK-3β in H9 cells in 15 minutes (Fig. 2A, 2B, 2C) as described previously [16,32]. Addition of GFX at 5.0 μM in the presence of FGF-2 significantly increased AKT phosphorylation in 15 minutes compared with addition of FGF-2 alone (Fig. 2A, 2B, Fig. S1E). The level of ERK-1/2 phosphorylation induced by FGF-2 with GFX was comparable with that without GFX (Fig. 2A). On the other hand, FGF-2-induced GSK-3β phosphorylation was completely inhibited by GFX (Fig. 2A, 2B) at concentrations higher than 1 μM treatment (Fig. S1E).

Addition of the PI3K inhibitor LY-294002 with FGF-2 completely inhibited AKT phosphorylation and significantly reduced GSK-3β phosphorylation (Fig. 2B, Fig. S1B). Addition of the MEK inhibitor U0126 with FGF-2 reduced ERK-1/2 phosphorylation and had little influence on GSK-3β phosphorylation. Addition of the GSK inhibitor BIO with FGF-2 signifi-

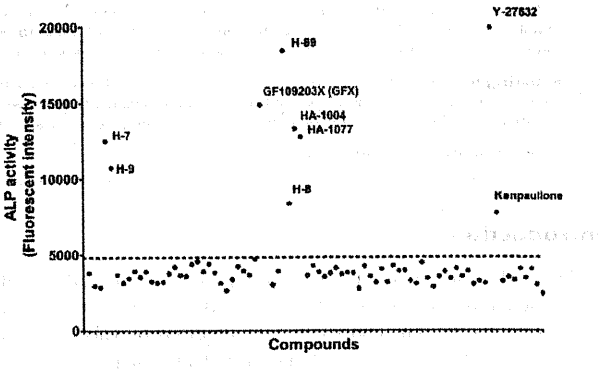

Figure 1. An ALP activity-based high-throughput screening assay of chemical library for PKC inhibitors. The ALP activity using 4-methylumbelliferyl phosphate [59] in 201B7 hiPS cells in a 96-well plate was measured by fluorometry. Each dot on the graph represents the fluorescent intensity for each compound of the kinase inhibitor library. Dotted line indicates the level for DMSO as a control.
doi:10.1371/journal.pone.0054122.g001

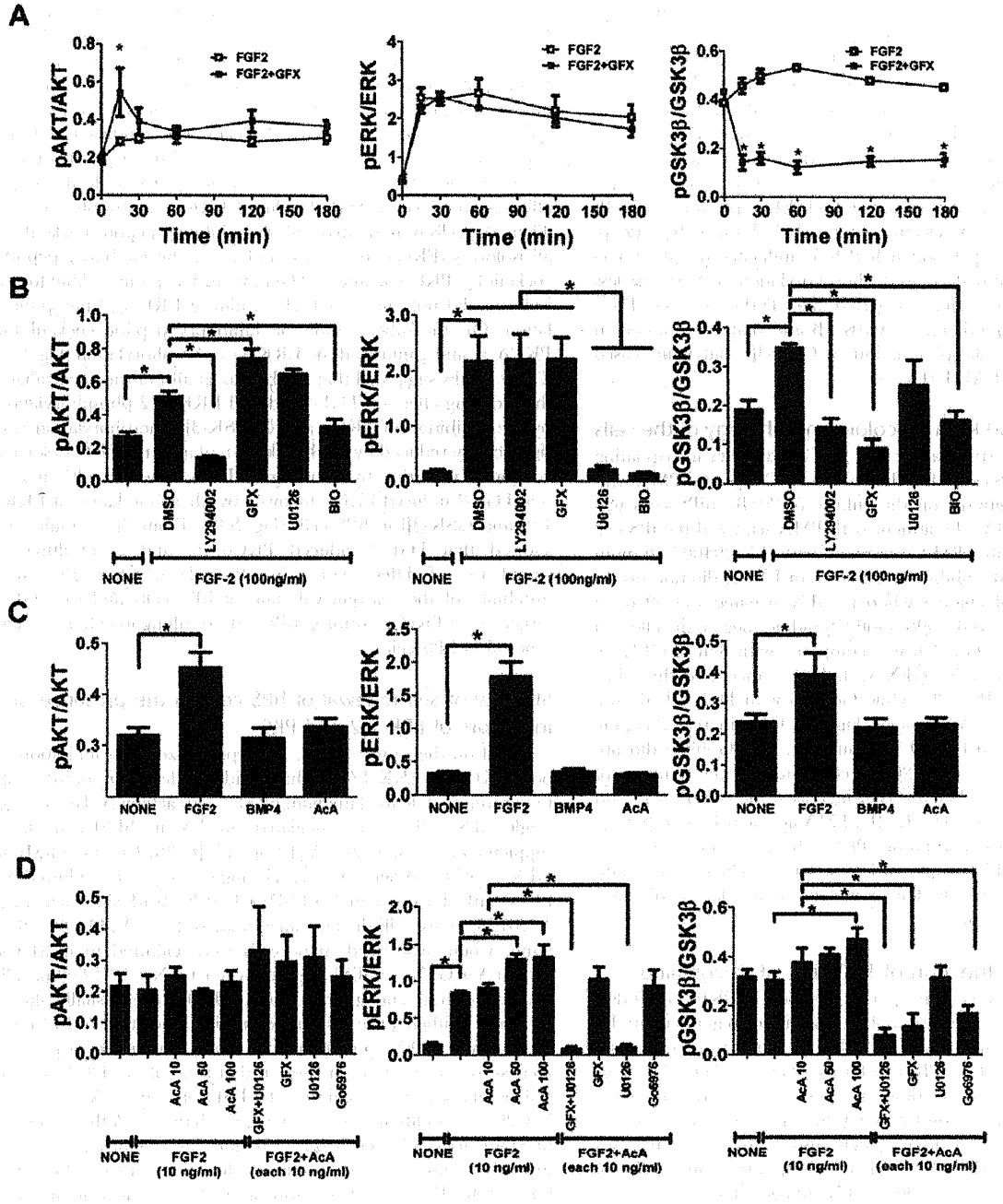

Figure 2. Effect of PKC inhibitor on FGF-2 signaling in hPS cells. The phosphorylation levels in H9 hES cells were measured by AlphaScreen® SureFire® assay kit. The values of the y-axis are the ratio of each phosphorylation to each total signal protein. (A) The cells were stimulated with FGF-2 (100 ng/ml) in fresh medium without insulin after overnight starvation and incubated with (open square) or without GFX (5 μM, closed square) for 180 minutes. The data are represented as means ± SE (n = 3). *P<0.05. (B) The cells were stimulated with FGF-2 (100 ng/ml) in fresh medium without insulin after overnight starvation. Fifteen minutes after FGF-2 addition together with each inhibitor as indicated on the panel. The data are represented as means ± SE (n = 3). *P<0.05. (C) The cells were treated with FGF-2 (100 ng/ml), BMP-4 (100 ng/ml) or activin A (100 ng/ml) in fresh medium without insulin after overnight starvation. Fifteen minutes after the addition of each growth factor as indicated on the panel. The data are represented as means ± SE (n = 3). *P<0.05. (D) The cells after growth factor starvation were stimulated with FGF-2 (10 ng/ml) and activin A (10 or 100 ng/ml) together with U0126 (5 μM) and GFX (5 μM) or Gö6976 (5 μM) in fresh medium without insulin for 15 minutes. Fifteen minutes after the addition of each growth factor/inhibitor as indicated on the panel. The data are represented as means ± SE (n = 3). *P<0.05.
doi:10.1371/journal.pone.0054122.g002

cantly reduced phosphorylation of not only AKT, but also ERK-1/2 and GSK-3β.

Neither BMP-4 nor activin A in the absence of FGF-2 induced the phosphorylation of AKT, ERK-1/2, or GSK-3β in 201B7 iPS cells (Fig. 2C, Fig. S1C). From our previous report that activin A acts synergistically with FGF-2 in stimulating the phosphorylation of ERK-1/2 [20], we speculated that activin A may increase the phosphorylation of GSK-3β synergistically with FGF-2. Addition

of increasing concentrations of activin A with FGF-2 increased phosphorylation of both GSK-3β and ERK-1/2 in a dose-dependent manner in H9 hES cells (Fig. 2D, Fig. S1D). Addition of U0126 with FGF-2 and activin A had little influence on phosphorylation of both AKT and GSK-3β, and completely inhibited phosphorylation of ERK-1/2. Addition of GFX together with U0126 in the presence of FGF-2 and activin A not significantly increased phosphorylation of AKT, while it completely inhibited phosphorylation of both ERK-1/2 and GSK-3β (Fig. 2D, Fig. S1D). A selective inhibitor of classical PKC (α, β, and γ isoforms) [29], Gö6976 had little influence on phosphorylation of AKT and decreased phosphorylation of GSK-3β less than GFX. These results suggested that FGF-2-induced PKC stimulated phosphorylation of GSK-3β and that GFX inhibited the PKC-induced phosphorylation of GSK-3β, but it increased phosphorylation of AKT (Fig. S2).

Effect of GFX and PMA on colony morphology of the cells

To confirm the speculation that PKCs play roles in regulating self-renewal in hPS cells, the effect of the PKC activator PMA with several kinase inhibitors on the culture of 201B7 hiPS cells was determined (Fig. 3A). Treatment with PMA scattered the iPS cell colony dramatically. PMA-treatment with LY-294002, lithium chloride (LiCl, GSK inhibitor), Y-27632, or U0126 did not reverse the morphological change whereas GFX negated the effect of PMA on cultured 201B7 cells. Gö6976 did not negate the effect of PKC. The effect of Gö6976 was compared with that of GFX on ALP-activity of the cells: GFX with FGF-2 increased the ALP-activity of 201B7 iPS cells, while Gö6976 with FGF-2 had little effect on ALP-activity of the cells (Fig. 3B). GFX increased colony forming efficiency in hESF9 medium (Fig. 3C). Gö6976 did not increase the colony sizes of 201B7 cells and also cell numbers of H9 and 201B7 cells whereas GFX increased the colony sizes and also cell numbers (Fig. 3D, 3E, 3F). PMA activates PKCα, β, γ, δ, ε, η, and θ whereas GFX inhibits PKCα, β, γ, δ, ε, and ζ isoforms. Gö6976 inhibits PKCα, β, and γ isoforms. These results and findings suggested that PKCδ or ε isoforms regulate undifferentiated state of hPS cells.

Isoform-specific function of PKCs in FGF-2 signaling

To determine the isoform-specific function of PKCs on FGF-2 signaling, at first the expression of 11 PKC isoform genes in 201B7 iPS cells was determined by RT-PCR. The results showed that the cells expressed all of 11 PKC isoforms examined here (Fig. 4A). The PKC inhibitor results described above suggested that PKCδ or PKCε might be responsible for GSK-3β phosphorylation but there is a possibility that PKCζ might also be involved. Then, we examined whether FGF-2 stimulated phosphorylation of PKCδ, PKCε or PKCζ with or without GFX. Image analysis of western blotting showed that the phosphorylation of PKCδ and PKCε was increased in a time-dependent manner after stimulation of FGF-2 and the phosphorylation of PKCζ was increased in 15 min after stimulation of FGF-2 and then decreased, suggesting that activation mechanism of PKCζ might be related with GSK-3β phosphorylation (Fig. 4B). GFX diminished the increased phosphorylation of all three PKCs. These result indicated that FGF-2 induced PKCδ, PKCε, and PKCζ in hPS cells.

We next examined the effects of short interfering RNA (siRNA) targeting PKCδ, PKCε or PKCζ on FGF-2 signaling in 201B7 iPS cells. The efficacy and specificity of siRNA was confirmed by quantitative RT-PCR (Fig. S3A). The expression of the targeted PKC genes was inhibited for at least 60%. The phosphorylation levels of AKT, ERK-1/2 and GSK-3β were measured in these PKCs-knockdown cells by AlphaScreen® SureFire® assay kit. The results showed that knockdown of PKCδ, and PKCζ did not affect FGF-2-induced AKT phosphorylation while knockdown of PKCε significantly reduced it (Fig. 4C). Knockdown of either PKCε or PKCζ isoform significantly decreased FGF-2-induced ERK-1/2 phosphorylation. GFX which is reported to target PKCα, β, γ, δ, ε and ζ isoforms did not change the level of FGF-2-induced ERK-1/2 phosphorylation, as shown above (Fig. 2 and Fig. S1). These results implied that cross-interaction among PKC isoforms might affect on the level of FGF-2-induced ERK-1/2 phosphorylation. Then, the cells were treated with the inhibitory peptide cocktail for all isoforms (PKCα, β, γ, δ, ε and ζ), or the inhibitory peptide cocktail for PKCδ, ε, and ζ. The inhibitory peptide cocktail for all isoforms did not affect on FGF-2-induced ERK-1/2 phosphorylation. On the other hand, the inhibitory peptide cocktail for PKCδ, ε, and ζ inhibited the ERK-1/2 phosphorylation (Fig. S4). These results suggested that inhibitions of all isoforms neutralized the reducing effect on FGF-2-induced ERK-1/2 phosphorylation by the inhibition of PKCε and ζ. GSK-3β phosphorylation was significantly reduced by the knockdown of all three PKC isoforms, compared with that by non-target siRNA. These results suggest that FGF-2 induced PKCs, followed by phosphorylation of ERK-1/2 and GSK-3β in hPS cells (Fig. S3B). From these results, we showed that FGF-2 induced PKCδ, ε, and ζ, resulting in stimulation of differentiation in hPS cells which might cause instability of the self-renewal state of hPS cells and that GFX targets these PKC isoforms in hPS cells, resulting in enhanced self-renewal of hPS cells.

Stability of self-renewal of hPS cells in the presence of inhibitors of ERK-1/2 and PKC

Based on the results above, we hypothesized that inhibition of both PKC and ERK-1/2 might provide stable culture of hPS cells in our minimal defined medium hESF9 with activin A. Dissociated single hPS cells were inoculated on FN in hESF9 medium supplemented with activin A (10 ng/ml) [8,20], U0126 (5 μM) or GFX (5 μM). When dissociated single cells were cultured in hESF9, hESF9 + activin A, hESF9 + U0126, or hESF9 + activin A + U0126, many cells died or differentiated (Fig. 5A). On the other hand, when dissociated single cells were cultured in hESF9 + activin A + GFX, or hESF9 + activin A + GFX + U0126 (2i), cells could proliferate enough to be passaged. However, usually after 3 passages, epithelial-like cells appeared in the culture of hESF9 + activin A + GFX condition (Fig. S5A). Immunocytochemical analysis by image analyzer showed that ratio of OCT3/4-positive cell population in the culture of hESF9 + activin A + GFX + U0126 (2i) condition was slightly higher than that in the culture of hESF9 + activin A + GFX (Fig. S5B and S5C). Gene expression in the cells cultured in these culture conditions was analyzed by real-time PCR (Fig. 5B). The expression of an endoderm marker, FOXA2, and a mesoderm marker, T were increased by activin A but it was significantly reduced by the addition of U0126. When the cells were cultured in hESF9 + activin A + U0126 + GFX, both FOXA2 and T were inhibited at lower level and also the undifferentiated makers, NANOG and OCT3/4 were maintained at higher ratio in the cells than those in other culture conditions. Next, the serial culture of dissociated single cells of hES H9, hES KhES4, hiPS 201B7 and hiPS Tic [33] cell lines were tested in hESF9 medium supplemented with activin A (10 ng/ml), U0126 (5 μM) and GFX (5 μM) (designated hESF9a_{2i} medium; Table S1). Dissociated single hPS cells were grown on FN in hESF9a_{2i} medium for 3 passages. Phase-contrast image showed that cell morphology seemed undifferentiated although they did not form hPS typical cell colony. OCT3/4 expression profiles were confirmed by immunofluorescence analysis using image analyzer,

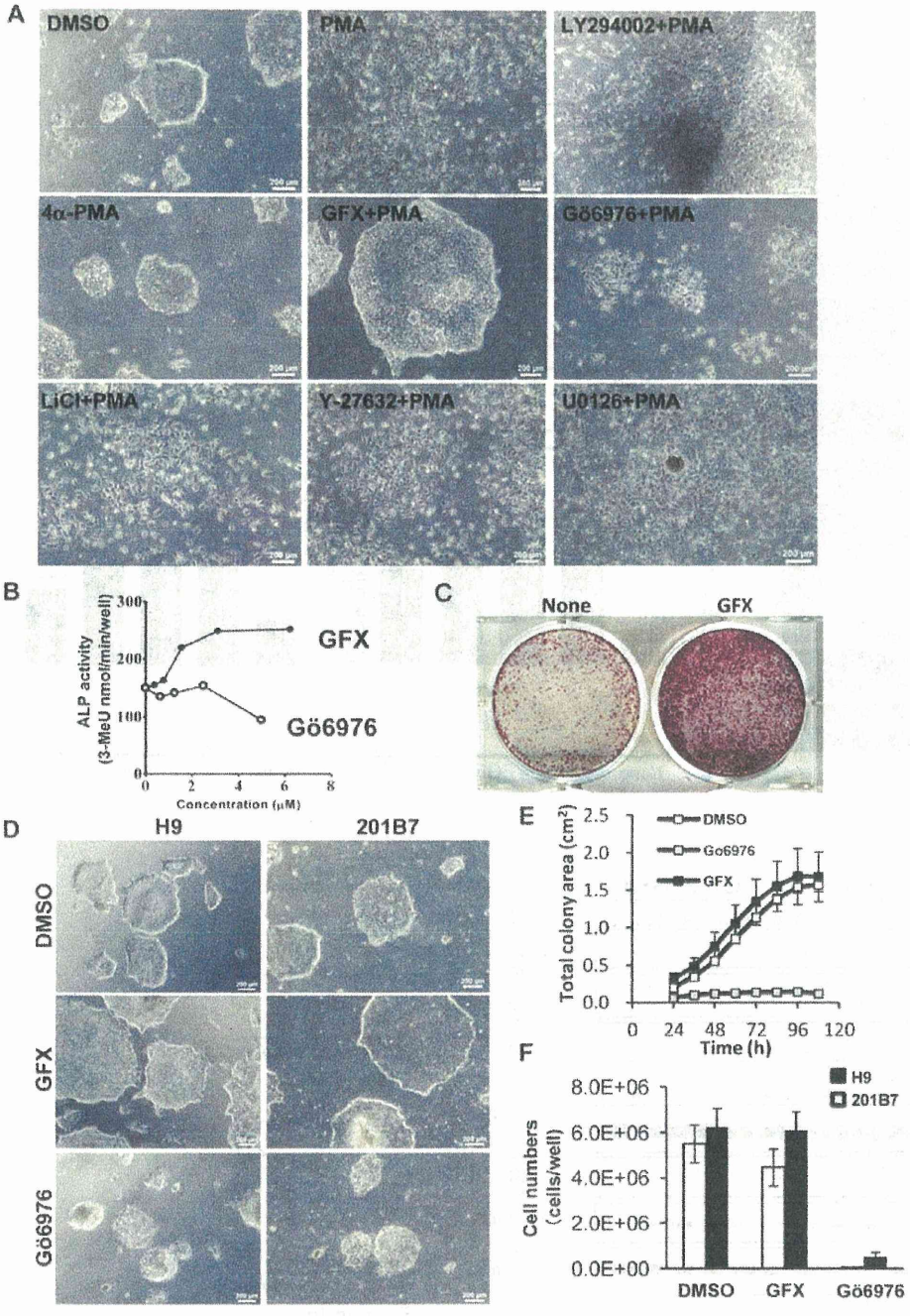

Figure 3. The effect of PKC on the morphologies of hPS cells with or without GFX. (A) Phase-contrast image of 201B7 hiPS cells cultured in feeder-free hESF9 defined medium on FN 24 hours after treatment with DMSO, PMA (10 nM), 4α-PMA (10 nM), GFX (5 μM), PMA (10 nM) with GFX (5 μM), PMA (10 nM) with Gö6976 (5 μM), PMA (10 nM) with LY-294002 (50 μM), PMA (10 nM) with LiCl (1 mM), PMA (10 nM) with Y-27632 (10 μM), or PMA (10 nM) with U0126 (20 μM). An inactive PMA analogue, 4α-PMA is used as negative control. Scale bars, 200 μm. (B) Quantitative ALP-based assay of 201B7 hiPS cells cultured in feeder-free hESF9 medium with GFX (closed circle) or Gö6976 (open circle) as indicated concentrations. (C) Colony forming efficiency of dissociated single hPS cells cultured with or without GFX. Dissociated single 201B7 cells seeded at 250,000 cells/well were grown on a 6-well plate coated with FN (2 μg/cm^2) in hESF9 medium supplemented with and without 1 μM GFX. A in 5 days and stained with ALP fast-red substrate. (D) Phase-contrast image of 201B7 hiPS cells or H9 hES cells cultured in feeder-free hESF9 medium with DMSO (open square), GFX (5 μM, gray square), or Gö6976 (5 μM, closed square). (E) Growth of cell colony area of hPS cells in the presence of GFX or Gö6976. The whole images of 201B7 cell colonies grown in a 6-well-plate coated with FN in the presence of DMSO, GFX or Gö6976 in hESF9 medium was measured by an analysis software, Cell-Quant. The images were captured every 12 hours in live cell imaging system Biostation CT. The data are represented as means ± SD (n = 3). (F) Cell growth of hPS cells in the presence of GFX or Gö6976. The numbers of H9 (open bars) and 201B7 cells (closed bars) grown in a 6-well-plate coated with FN in the presence of DMSO, GFX or Gö6976 in hESF9 medium were counted on 5 days. The data are represented as means ± SD (n = 3).

doi:10.1371/journal.pone.0054122.g003

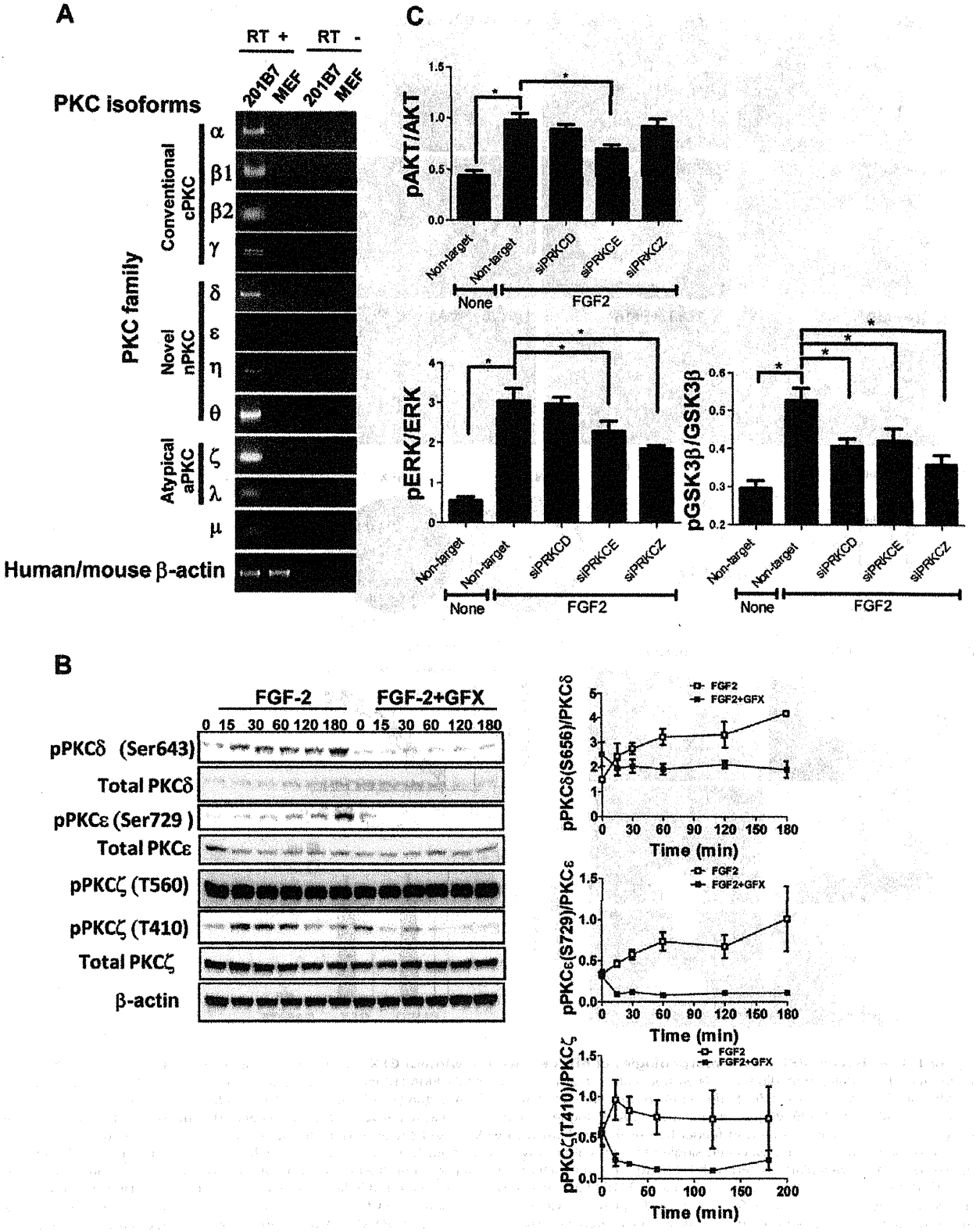

Figure 4. Specific-isoform of PKCs function in FGF-2 signaling. (**A**) RT-PCR analysis of PKC isoform expression. Total RNA was extracted from the undifferentiated 201B7 hiPS cells cultured on feeder cells (CF-1) with KSR-based medium or the feeder cells. Primers were listed in Table S3. (**B**) Phosphorylation of PKCδ, ε, or ζ isoforms induced by FGF-2 (open square) with GFX (closed square). 201B7 hiPS cells were stimulated with FGF-2 (100 ng/ml) after overnight starvation and incubated with or without GFX (5 μM) for 180 minutes. The cells were lysed and followed by western blot

analysis using an antibody detecting the phosphorylation or total protein amount of PKCδ, PKCε, or PKCζ. Protein content quantified from the gel blot images (n = 3). The values of the y-axis are the ratio of each phosphorylation to each total signal protein. (**C**) FGF-2 signaling in hPS cells with specific PKC isoforms-targeting siRNA. 201B7 iPS cells were transfected with specific PKCδ, ε, or ζ isoforms-targeting siRNA or non-targeting siRNA. The phosphorylation levels of the cells treated with FGF-2(100 ng/ml) after overnight starvation were measured by AlphaScreen® SureFire® assay kit. The values of the y-axis are the ratio of each phosphorylation to each total signal protein. The data are represented as means ± SE (n = 3). *P<0.05.
doi:10.1371/journal.pone.0054122.g004

suggesting that the hPS cells maintained undifferentiated state. Another undifferentiated maker, TRA-1-60 expression was also confirmed in hPS cells grown in hESF9a_{2i} medium for 3 passages (Fig. S6).

Serial culture more than 10 passages of undifferentiated H9 hES cells and 201B7 hiPS were tested on FN in hESF9a_{2i} medium. Undifferentiated morphologies of 201B7 hiPS (Fig. S7A) and H9 hES colonies (Fig. S8A) were maintained for more than 30 passages using the conventional passage procedure. The growth rates of H9 hES and 201B7 hiPS cells in hESF9a_{2i} medium were similar to those of cells grown in the conventional KSR-based medium on feeders (Figs. S7B and S8B). The cells retained expression of stage-specific embryonic antigen (SSEA)-4 [34], cell surface antigens TRA-1-60 [35], TRA-1-81 [35], CD90 (Thy-1) [36], and TRA-2-54 [36] (alkaline phosphatase), but did not express SSEA-1 [37] or a neural marker A2B5 [36] (Fig. S7C, S7D and S8C, S8D). The cells retained normal karyotypes (Fig. S9A), pluripotency in vitro (Fig. S9B) and in vivo (Fig. S9C). These results confirmed that inhibition of both ERK-1/2 and PKC supported the self-renewal of hPS cells.

Discussion

Many studies reported that FGF-2 activates both the MAPK/ERK, and PI3K/AKT pathways, which are important for maintaining pluripotency and viability in hPS cells [9,14–16]. However, FGF-2 downstream signaling is not clearly understood in hPS cells. In this study using a minimum essential defined culture system [8,20], we showed that FGF-2 activated PI3K/AKT and MEK/ERK-1/2, but also PKCδ, ε and ζ isoforms in hPS cells (Fig. 6).

The PKC family has been implicated as an intracellular mediator of several neurotransmitters, hormones, tumor promoters, α1-adrenergic agonists, and phorbol esters, and it is important in the regulation of growth, differentiation, cell death, and neurotransmission [38]. The PKC family comprises classical (PKCα, β, and γ; activated by Ca^{2+} and phorbol esters), novel PKC (PKCδ, ε, η, and θ; activated by phorbol esters but not regulated by Ca^{2+}), and atypical PKC (PKCζ and PKCι/λ; not activated by Ca^{2+} or phorbol esters). Different isoforms may perform distinct functions, as suggested by their differential pattern of localization, differences in condition of activation, and some differences in substrate specificity [39–40]. PKC has previously been implicated in GSK-3 regulation [41–42]. Fang et al. [43] showed that PKCα, βII, γ, η, and δ were capable of phosphorylating GSK-3β while PKCε and PKCζ did not phosphorylate GSK-3 by in vitro kinase assays; also, expression of constitutively active PKCα, βI, γ, η enhanced phosphorylation of cotransfected GSK-3β in HEK293 cells. On the other hand, Eng et al. [15] reported that negative construct of PKCε isoform prevented phosphorylation of GSK-3 in migrating fibroblasts. These pieces of evidence suggested that specific isoforms of PKC have different roles in different types of cells. Shuibing et al. [44] reported that activation of PKCα and/or β directs the pancreatic specification of hES cells. Recently, Feng et al. [45] reported that activation of PKCδ induces extraembryonic endoderm differentiation of hES cells. These studies suggested that PKCs might be involved in differentiation of hPS cells. Our study showed that FGF-2 induced PKCδ, ε, and ζ, resulting in phosphorylation of GSK-3β, ERK-1/2, or AKT. Chou, et al. [46] reported that the phosphorylation of PKCζ was regulated by PI3-kinase and PDK-1 in NIH 3T3 fibroblasts. Intriguingly, PKCζ can stimulate GSK-3 activity, by relieving PKB-imposed inhibition [47]. In mouse ES cells, it has been shown that PKCζ plays an important role in inducing lineage commitment in mESCs through a PKCζ–nuclear factor kappa-light-chain-enhancer of activated B cells signaling axis [48]. However, PKC inhibition does not change phosphorylation of ERK-1/2 or GSK-3β. In view of the fact that LIF mainly regulates self-renewal in mouse ES cells, isoform specific function might be cross-regulated by other signaling in the cells. Further, our study showed that the combination effect by inhibition of PKCα, β, γ, δ, ε, and ζ was different from that by inhibition of PKCε and ζ, suggesting that each PKC might interact in different contexts and also PKCδ, ε, and ζ might have different activation mechanisms in hPS cells. It is needed further investigation in future.

GSK-3β is inhibited by phosphorylation stimulated by the canonical Wnt signal pathway, which is followed by the accumulation of β-catenin to the nucleus [49]. From the above findings, it follows that FGF-2 may activate Wnt signaling through PKC leading to differentiation of hPS cells. This conclusion contradicts the findings of previous studies demonstrating that canonical Wnt signaling supports self-renewal of stem cells [50–52]. However, it is consistent with a study showing that canonical Wnt signaling does not appear to promote stem cell maintenance, which prevents differentiation of stem cells [53]. On the other hand, some studies have shown a dual function for Wnt signaling in hES cells in that the pathways of self-renewal or differentiation are dependent on the presence of hES cell supporting factors [51–52]. Recently, Ding et al. [32] showed that FGF-2 modulates Wnt signaling through AKT/GSK-3β signaling and suggested that the differences in the results could be due to the culture platform. Our findings suggest that GSK-3β activity is regulated by FGF-2 through both PI3K/AKT and PKC pathways. AKT/GSK-3β signaling may support self-renewal whereas PKC/GSK-3β may promote cell differentiation of hPS cells. However, GFX decreased the phosphorylation level of GSK-3β to lower level than non-treatment. GSK-3β signaling might be stimulated also by other signal pathway in hPS cells. Target genes of these pathways and further regulation mechanisms in GSK-3β signaling should be analyzed in future.

TGF-β/activin/nodal pathways are thought to crosstalk with FGF signaling in regulating hPS cells. Vallier et al. [1–2,54] demonstrated that activin/nodal pathway in co-operation with FGF-2 is necessary for the maintenance of pluripotency in hES cells. We recently reported that activin A enhances FGF-2-induced ERK-1/2, which permits neural and mesendodermal differentiation of hES cells [20]. In this study we showed that activin A enhanced FGF-2-induced phosphorylation of not only ERK-1/2 but also GSK-3β. Inhibition of these pathways provided stable culture of hPS cells for long-term. In this study, we used both GFX and U0126 to inhibit these pathways. GFX targeting all of PKCα, β, γ, δ, ε, and ζ had no inhibitory effect on ERK-1/2 pathway although siRNA targeting PKCε or PKCζ decreased it. If more specific inhibitor is developed in future, it would be more useful.

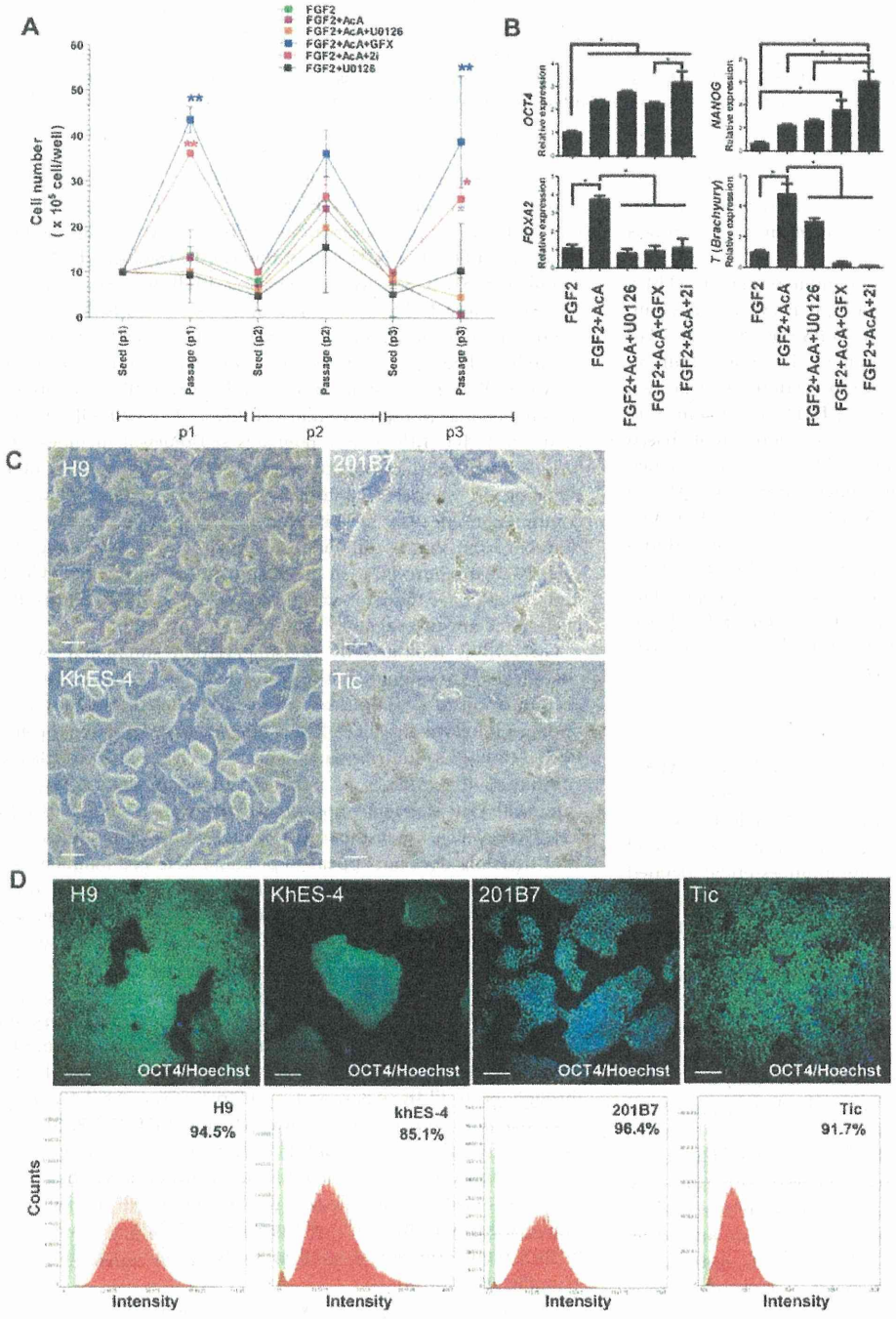

Figure 5. Single cell culture of hPS cells in the hESF9a$_{2i}$ medium. (A) Cell growth of dissociated single H9 hES cells cultured in each indicated condition for three passages. Cells were reseeded at the cell density of 1×10^6 cells/well every 5 days. When the cells were passages, cell numbers were counted. Cell growth in the hESF9a$_{2i}$ medium was significantly different ($P<0.05$) from hESF9 (FGF-2), FGF-2 + activin A, FGF-2 + activin A + U0126. Cell growth in hESF9a + GFX was significantly different ($P<0.05$) from hESF9 (FGF-2), FGF-2 + activin A, FGF-2 + activin A + U0126, and FGF2 + U0126. The data are represented as means ± SE (n = 3). (**B**) Gene expression in the hPS cells cultured in each indicated condition for three passages. The gene expression levels of NANOG, OCT3/4, FOXA2, T in the cells were measured by real-time RT-PCR. On the y axis, the gene expression level in the cells cultured with FGF-2 in a experiment was taken as 1.0. The data are represented as means ± SE (n = 3). *$P<0.05$. (**C**) Phase-contrast image of hPS cells grown on FN in hESF9a$_{2i}$ medium for 3 passages. The cells were dissociated into single cells for passage, and reseeded at a ratio of 1:3 - 1:5 every five days. Scale bars, 200 μm. (**D**) OCT3/4 expression in hPS cells grown on FN in hESF9a$_{2i}$. The cells grown in hESF9a$_{2i}$ as described above in Figure 5C were reseeded on a 6-well-plate and cultured for 5 days. The cells stained with anti-OCT3/4 antibody were visualized with Alexa Fluor 488 (upper panels). Nuclei were stained with Hoechst 33342 (blue). Scale bars, 200 μm. Whole cell images in whole plate were captured and OCT3/4 expression profiles were analyzed by Image Analyzer (lower panels). Antigen histogram (red); control histogram (green); Y axis is cell numbers and X axis is fluorescence intensity for anti-OCT3/4 antibody.

doi:10.1371/journal.pone.0054122.g005

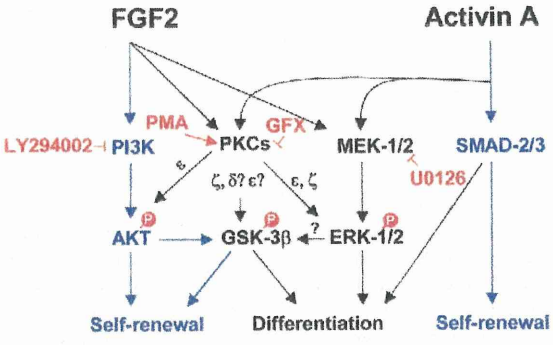

Figure 6. Model for the molecular mechanism of PKCs regulating self-renewal or differentiation in hPS cells. Our study suggested a model that FGF-2 activates PI3K/AKT, MEK/ERK-1/2, and PKCε/δ/ζ. PKCε, δ, and ζ inactivates directly or indirectly GSK-3β by phosphorylation which promotes differentiation of hPS cells. PKCε and ζ activates ERK-1/2 which promotes differentiation of hPS cells. Activin A activates SMAD-2/3 which controls self-renewal and differentiation while activin A together with FGF-2 activates both ERK-1/2 and PKCs. Inhibition of both ERK-1/2 and PKCs pathway provides a metastable undifferentiated state of hPS cells. Blue arrow indicated pathway promoting hPS cell self-renewal and black arrow indicated pathway promoting hPS cell differentiation.
doi:10.1371/journal.pone.0054122.g006

To maintain undifferentiated state, balancing among ERK-1/2, PI3K, SMAD, and PKC signal pathways may be required in any culture conditions. KSR of which components are not disclosed in public is known to have BMP-4-like activity [55]. Some components including BMP-4 in KSR together with secreting factors from mouse feeders might regulate PKC/ERK-1/2 signaling. Using our defined conditions, more molecules including growth factors would be screened to detect their accurate effects on hPS cells.

In conclusion, our study suggested that FGF-2 induced PI3K/AKT and MEK/ERK-1/2, but also PKCs in hPS cells. PI3K/AKT promotes cell self-renewal whereas the MEK/ERK-1/2, PKC/ERK-1/2 and PKC/GSK-3β pathways down-regulate hPS cell self-renewal. This study helps to untangle the cross-talk between molecular mechanisms regulating self-renewal and differentiation of hPS cells.

Materials and Methods

Chemicals

A chemical library of kinase inhibitors (Biomol, Plymouth Meeting, PA, USA), LY-294002 (Cell Signaling Technology, Beverly, MA, USA), BIO (Merck, Darmstadt, Germany), U0126 (Promega, Madison, WI, USA), Y-27632 (Wako Pure Chemical, Osaka, Japan), PMA (Sigma, St. Louis, MO, USA), 4α-PMA (Promega) and Gö6976 (Sigma) were dissolved in dimethyl sulfoxide (DMSO). LiCl (Sigma) and GF109203X hydrochloride (Sigma) were dissolved in water.

PKC inhibitory peptides

Membrane-permeable PKCδ inhibitory peptide δV1-1 (SFNSYELGSL: amino acids 8-17 of PKCδ) or PKCε inhibitory peptide εV1-2 (EAVSLKPT: amino acids 14-21 of PKCε) were designed according to the method of Mochly-Rosen [56–57]. The peptides were custom-synthesized by Sigma (purified to >95% by HPLC). Myristoylated PKCα, β, and γ inhibitory peptide and myristoylated PKCζ inhibitory peptide were purchased from Promega and Calbiochem (Darmstadt, Germany), respectively.

Cell culture

The hES cell lines, H9 [10,31] (WA09, WISC Bank, WiCell Research Institute, Madison, WI, USA) and KhES-4 (provided by Kyoto University, Kyoto, Japan), and hiPS cell lines, 201B7 [26] (provided by Dr. Shinya Yamanaka, Kyoto University) and Tic (JCRB1331, JCRB Cell Bank, Osaka, Japan) [33,58] were routinely maintained on mitomycin C-inactivated mouse embryo fibroblast feeder cells (MEF, Millipore Co., Billerica, MA, USA) in an KSR-based medium supplemented with 5 ng/ml (H9, khES-4), 4 ng/ml (201B7) or 10 ng/ml (Tic) human recombinant FGF-2 (Katayama Kagaku Kogyo LTD., Osaka, Japan) previously described [10]. Human ES cells were used following the Guidelines for utilization of human embryonic stem cells of the Ministry of Education, Culture, Sports, Science and Technology of Japan after approval by the institutional ethical review board at National Institute of Biomedical Innovation. The cells were passaged with 1 mg/ml dispase (Roche, Mannheim, Germany) in DMEM/F12 medium and a plastic scraper (Sumitomo Bakelite Co., LTD Tokyo, Japan). The cells were split at a ratio of 1:5–1:8 every 5 days.

Human ES/iPS cell culture in feeder-free and growth factor defined serum-free medium

Prior to culture in feeder-free conditions, the medium was changed from the KSR-based medium to a growth factor-defined serum-free hESF9 medium [8] (Table S1). Two days after the medium change, the cells were harvested with 1 mg/ml dispase or TrypLE (Invitrogen), and reseeded on plastic plates coated with bovine FN (Sigma, 2 μg/cm^2) [21]. For long-term culture, hPS cells were maintained on FN in hESF9 medium supplemented with 10 ng/ml human recombinant activin A (R&D Systems Minneapolis, MN, USA) in the presence of both 5 μM U0126 [20], and 5 μM GFX, designated hESF9a$_{2i}$ medium. The medium was changed every day.

Single hPS cell culturing with two inhibitors

hPS cells were dissociated with TrypLE (Invitrogen) into single cells, and seeded on a 6-well plate coated with FN at the cell density of 1×10^6 cells/well in hESF9, or supplemented with 10 ng/ml activin A, 5 μM U0126, or 5 μM GFX. The medium was changed every day.

Quantitative ALP activity-based high-throughput screening assay

The hPS cells were dissociated with accutase into single cells and seeded at 5×10^4 cells/well on a 96-well plate coated with FN (FN, 2 μg/cm^2) in hESF9 medium. Each compound in the chemical library was added at 2.5 μM to each well. After further 5 days-culture, the cells were washed with 3-[4-(2-Hydroxyethyl)-1-piperazinyl] propanesulfonic acid (EPPA) buffer (30 mM, pH 8.2). Fluorescence ALP substrate (0.2 mM, 4-methylumbelliferyl phosphate) [59] in EPPS buffer was added into the wells. After incubation for 30 min at 37°C, EPPS buffer (100 mM, pH 7.7) supplemented with 1 M K_2HPO_4 was add to terminate the enzyme reaction. The amount of 4-methylumbelliferone (4-MeU) produced via the enzyme reaction was measured with a fluorescence microplate reader (Gemini EM, Molecular Devices, Menlo Park, CA). The specific activity of ALP was quantified by reference to a standard fluorescence curve generated with known concentrations of 4-MeU (Sigma).